Biomedical Microdevices (2021) 23: 43
https://doi.org/10.1007/s10544-021-00581-0

Cellulose nanocrystals-based materials as hemostatic agents for wound dressings: a review

Anne Carolyne Mendonça Cidreira[1] · Karine Cappuccio de Castro[1] · Tahmasb Hatami[1] · Lamia Zuniga Linan[2] · Lucia Helena Innocentini Mei[1]

Accepted: 28 August 2021 / Published online: 7 September 2021

Abstract

Wound dressings are devices used to stop bleeding and provide appropriate environmental conditions to accelerate wound healing. The effectiveness of wound dressing materials can be crucial to prevent deaths from excessive bleeding in surgeries and promote complete restoration of the injury. Some requirements for an ideal wound dressing are rapid hemostatic effect, high swelling capacity, antibacterial properties, biocompatibility, biodegradability, and mechanical strength. However, finding all these properties in a single material remains a challenge. In this context, nanocomposites have demonstrated an excellent capacity for this application because of their multifunctionality. One of the emerging materials used in nanocomposite manufacture is cellulose nanocrystals (CNCs), which are rod-like crystalline nanometric structures present on cellulose chains. These nanoparticles are attractive for wound healing applications because of their high aspect ratio, high mechanical properties, functionality and low density. Hence, this work aimed to present an overview of nanocomposites constituted by CNCs for wound healing applications. The review focuses on the most common materials used as matrices, the types of dressing, and their fabrication techniques. Novel wound dressings composites have improved hemostatic, swelling, and mechanical properties compared to other pure biopolymers while preserving their other biological properties. Films, nanofibers mats, sponges, and hydrogels have been prepared with CNCs nanocomposites, and in vitro and in vivo tests have proved their suitability for wound healing.

Keywords Wound dressings · Hemostasis · Nanocomposites · Cellulose nanocrystals (CNCs)

1 Introduction

Wound dressings are essential materials to stop bleeding in surgeries and promote hemostasis. They act as a barrier and control the oxygen and moisture crossing to the wound (Moohan et al. 2020). Hemostatic agents for wound healing must have specific properties such as a rapid hemostasis action, biocompatibility, nontoxicity, no antigenicity, easy degradation in vivo, tunable mechanical properties, good swelling ratio, low cost, and easy processing (Yang et al. 2017; Zhang et al. 2020; Ghobril and Grinstaff 2015). The primary biological hemostatic materials of available commercial products are thrombin, fibrin, collagen, gelatin matrix and albumin, polysaccharides such as chitosan, starch, oxidized cellulose (OC) and alginate, synthetic polymers such as polyethylene glycol and cyanoacrylates, and inorganic based materials such as smectite and kaolin (Yang et al. 2017; Behrens et al. 2014).

✉ Anne Carolyne Mendonça Cidreira
cidreiraanne22@gmail.com

Karine Cappuccio de Castro
cappuccio.karine@gmail.com

Tahmasb Hatami
thatami@unicamp.br

Lamia Zuniga Linan
lamiazuniga@yahoo.com.mx

Lucia Helena Innocentini Mei
lumeibit@unicamp.br

[1] Department of Material Engineering and Bioprocesses, University of Campinas (UNICAMP), School of Chemical Engineering (FEQ), University City Zeferino Vaz, Campinas, SP CEP 13083-970, Brazil

[2] Laboratory of Materials and Process Engineering (LaMEP), Chemical Engineering Department (DEEQ), Federal University of Maranhão (UFMA), Av. dos Portugueses, 1933, Bacanga, São Luís, MA CEP 65080-805, Brazil

Among them, oxidized cellulose-based hemostatic materials such as oxidized regenerated cellulose (ORC) are one of the most widely used topical hemostatic agents for internal bleeding control (Yuan et al. 2020). ORC is effective for major bleeds due to its ability to absorb considerable amounts of blood, more than multiple times its weight. (Cheng et al. 2013). Other advantages are easy handling, bactericidal effect, best times for clotting formation, and complete degradation in a period between 14 to 30 days (Cheng et al. 2016a; Khoshmohabat et al. 2019; Chen et al. 2020). However, some drawbacks related to ORC have been reported. Some examples are cases of inflammatory reactions caused by low pH due to the presence of acid carboxyl groups and erroneous postoperative diagnosis due to the appearance of a mass mimicking an abscess in ultrasound images when the ORC is left in situ (Piozzi et al. 2018).

Recently, the development of novel hemostatic materials based on nanocelluloses has been performed, mainly because of their high surface to volume ratio and the possibility of being incorporated into other materials to improve the hemostatic action and the wound healing process (Khoshmohabat et al. 2019; Moohan et al. 2020; Nakielski and Pierini 2019). Furthermore, nanocelluloses are renewable materials with high availability and relatively low cost as they can be obtained from different biomass sources (Bacakova et al. 2019).

Cellulose nanocrystals (CNCs), or cellulose nanowhiskers, are crystalline nanostructures stabilized by complex hydrogen bond interactions and dispersed in amorphous regions of cellulose (Habibi et al. 2010). This type of nanocellulose possesses biodegradable and biocompatible properties, high elastic modulus, nanoscale dimensions, high aspect ratio, low density, and a large number of hydroxyl groups on its surface that makes it suitable for chemical modifications (Gopi et al. 2019). Much work has been done with the applications of cellulose nanocrystal-based materials for wound dressings. However, a review covering the most common materials used as matrices, the types of dressing, and their fabrication techniques all together has not been published in the literature yet. So, this work attempts to address this gap by reviewing the most critical reported papers on fabricating CNCs-based nanocomposites for wound healing applications.

2 CNCs sources and properties

Cellulose nanocrystals can be obtained from different sources, and their properties vary due to the significant differences between biosynthesis processes of raw materials, which affect the cellulose chain stacking (Foster et al. 2018). The primary sources used to isolate these nanoparticles are lignocellulosic biomass as wood pulp, agricultural wastes and natural fibers, and more pure sources such as microcrystalline cellulose, algal cellulose and bacterial cellulose (Mokhena and John 2020).

Wood pulp is derived from two types of industrial process: (a) kraft process, which is performed with a mixture of sodium hydroxide and sodium sulfide (NaOH and Na_2S), and (b) sulphite pulping, using various salts of sulfurous acid (mostly sodium bisulphate $NaHSO_3$ or sodium sulphate Na_2SO_3) to remove the lignin content of the hard and softwood (Leppänen et al. 2009). In wood sources, the cellulose content is about 40–50%, and the CNCs obtained from this raw material presents a degree of crystallinity between 50 and 83%, which are lower than other sources, but with shorter dimensions (100–300 nm of length and 3–5 nm of diameter) (Gopi et al. 2019; Beck-Candanedo et al. 2005).

Agricultural waste and natural fibers have been used to extract cellulose nanocrystals, and they have received significant attention for waste managing, exploring eco-friendly resources, low cost, and availability (Golbaghi et al. 2017; Rajinipriya et al. 2018; Linan et al. 2021). Usually, the non-woody sources contain less lignin than the wood sources, and the microfibrils are less tightly bound in the structure of the cell walls. Therefore, the extraction of CNCs from these sources employs less strong chemical and mechanical treatments than those applied to wood sources (Trache et al. 2017).

Microcrystalline cellulose (MCC) is a purified form of cellulose obtained by acid hydrolysis with inorganic acids. MCC from wood pulp is commercially available as the trade name of Avicel®, a white powder with a size between 10–50 μm. Cellulose pulp is partially depolymerized in the susceptible amorph regions to liberate the microcrystalline form of cellulose (Hindi 2017). MCC is used to isolate CNCs by different methods, such as those described in Sect. 3 of this work.

Cellulose microfibrils may be found in the wall cells of different species of algae (green, grey, red, yellow-green, etc.) (Moon et al. 2011). Green algae species such as *Caldophora* and *Valonia* have been more explored due to the exceptionally high degree of crystallinity of their nanocellulose (about 95%, obtained from XRD). Moreover, in contrast with plant cellulose, this presents solitary rosettes of six hexagonally arranged subunits which generates thin microfibrils with random orientation (Mihranyan 2010). In addition, the green algae cellulose possesses a linear type arrangement capable of producing very thick microfibrils with a high degree of orientation (Mihranyan 2010). Because of these properties, it is used in biomedical and pharmaceutical applications as well as in composites and in the manufacture of paper filters and dialyzer membranes (Liu et al. 2017; Mihranyan 2010). Furthermore, algae nanocellulose differs from plant nanocellulose in dimension due to its micrometric scale length (Table 1).

Table 1 Dimensions and degree of crystallinity of CNCs from different sources of cellulose using sulfuric acid hydrolysis

Source	Length (nm)	Width (nm)	Degree of crystallinity (%)	References
Wheat straw	120–600	15–20	71	Oun and Rhim (2016)
Rice straw	130–650	12–20	66.3	Oun and Rhim (2016)
Maize husk	940 ± 70	6 ± 2	51.66	Smyth et al. (2017)
Coconut fiber	208 ± 34	4.9 ± 0.5	80	Nascimento et al. (2016)
Sugarcane bagasse	200–300	20–40	68.28	Sukyai et al. (2018)
Green algae	600	10–30	95	Mihranyan (2010)
Bacterial	622 ± 100	33.7 ± 14	83–91	Vasconcelos et al. (2017)
Microcrystalline cellulose	270 ± 122	17 ± 8	85.5	Du et al. (2017)

Certain bacteria synthesize bacterial cellulose (BC) as the Azotobacter, Pseudomonas, Salmonella and Sarcina ventriculi genera (de Fernandes et al. 2020). BC is extracted in a purer form compared to cellulose from lignocellulosic biomass because of the absence of other compounds found in plant cells structure such as lignin, hemicellulose, and other carbohydrates (Jozala et al. 2016). The mechanism of BC synthesis consists of the same steps as any other organisms, including plants, which is the formation of β−1 → 4 glucan chain with the polymerization of glucan units, and assembly and crystallization of cellulose chain (Fig. 1). Nevertheless, the degree of polymerization differs from about 13,000 to 14,000 for plants and 2000 to 6000 for BC (Chawla et al. 2009).

Nanocrystals can be obtained from BC by acid hydrolysis and, depending on the reaction conditions, CNCs from this source can reach a high degree of crystallinity, as shown in Table 1 (Vasconcelos et al. 2017).

3 Preparation methods of CNCs

CNCs are aleatorily distributed in the cellulose chain and connected by amorph regions. Chemical, mechanical, or even enzymatic treatments can isolate CNCs by disintegrating the disordered chains and preserving the crystal structure simultaneously (Fig. 2). Amorph chains are more susceptible

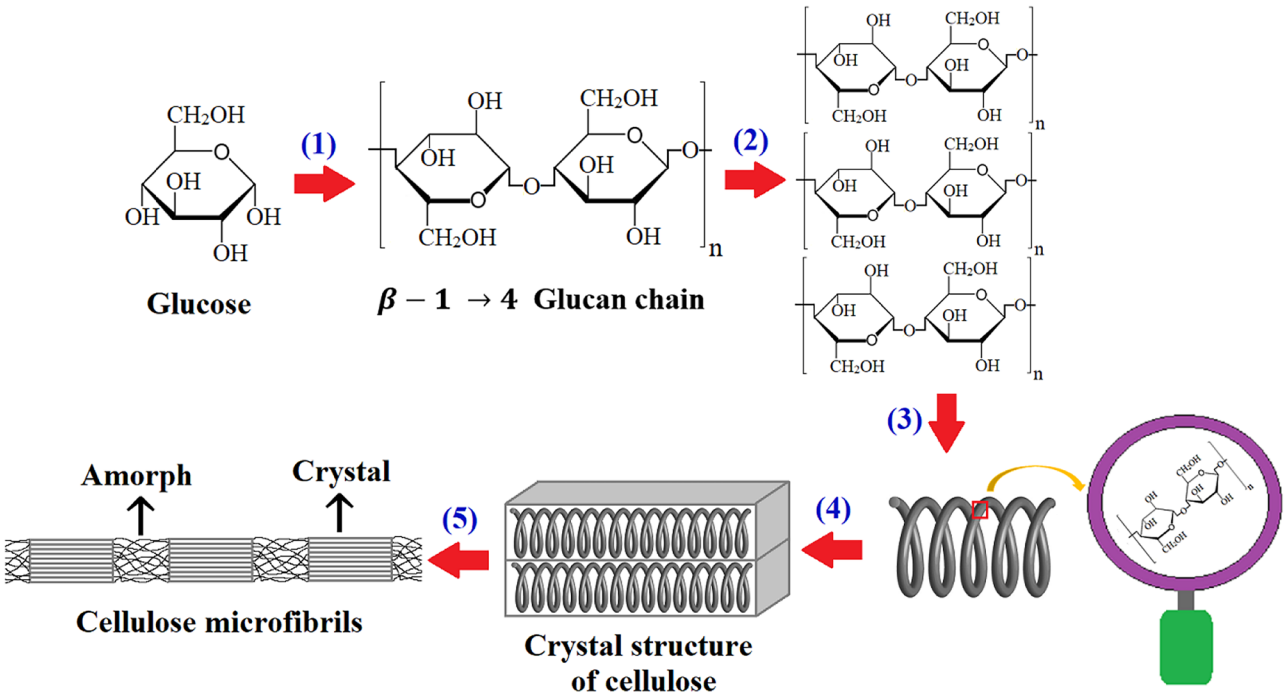

Fig. 1 Schematic representation of cellulose synthesis steps in organisms (plants, bacterial, algae etc.). (1) polymerization of glucose units by the formation of $\beta-1\rightarrow4$ linkage, (2) assemble of glucan chains to form cellulose molecule, (3) entanglement of cellulose molecules into thin fibrils, (4) crystallization of cellulose fibrils and (5) arrangement of cellulose microfibrils on crystal and amorph phase

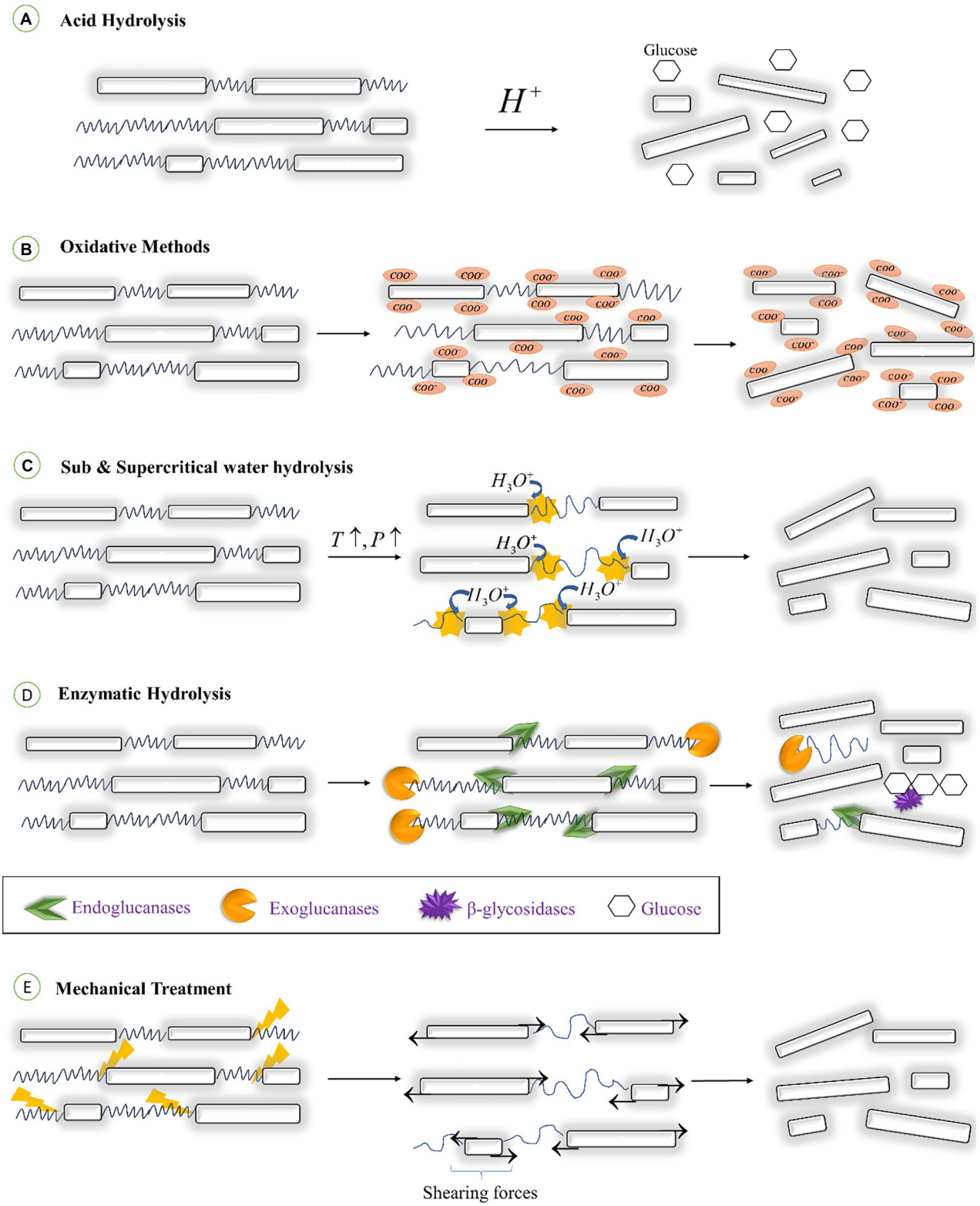

Fig. 2 Schematic representation of the mechanisms applied on CNC extraction methods. **A** Acid hydrolysis—protonated species (H^+) disrupt amorphs regions liberating CNCs and degraded sugars, **B** oxidative methods (ex. APS and TEMPO oxidation)—oxidant agents convert alcoholic groups on the surface of cellulose chain into carboxyl groups (COO^-), these anionic charges create repulsive forces that break amorphs chains, **C** sub and supercritical water hydrolysis—at high pressure and temperature the concentration of reactive hydronium ion increases and breakdown amorphs regions of cellulose, **D** enzymatic hydrolysis uses cellulases to disrupt the amorph phase and liberate crystals and **E** mechanical treatments—shearing forces fracture cellulose amorph chains and isolate CNCs

to disruption due to weaker hydrogen bond interactions operating in that region (Moon et al. 2011).

The CNC preparation methods can be classified into two general groups, namely conventional and green methods, explained as follows.

3.1 Conventional preparation method

One of the conventional methods widely applied to isolate CNCs from diverse sources is acid hydrolysis because of its high efficiency on the cleavage of C–O linkage of amorph chains. According to Xiang et al. (2003) researchers, protons H^+ released by the reactant interact with cellulose glycosidic bonds forming a conjugated acid, then, the cleavage of C-O linkage occurs, and the free sugars are removed in the presence of water (Fig. 2a).

Strong inorganic acids such as sulfuric acid, hydrochloric acid, and phosphoric acid can isolate CNCs with high crystalline index and small dimensions (Vanderfleet et al. 2018; Pereira et al. 2020; Arserim-Uçar et al. 2021).

The reaction using sulfuric acid incorporates sulfate groups on CNC's surface, which permits a good dispersion in an aqueous medium but affects thermal stability and promotes CNC's degradation at high temperatures (Kargarzadeh et al. 2018). Conversely, hydrochloric acid hydrolysis produces CNCs with high thermal stability because it does not introduce any sulfate group on CNC's surface. However, the lack of anionic charges in the medium facilitates CNCs agglomeration, and it might compromise their nanometric properties (Nagarajan et al. 2021).

Despite the current broad applicability, these acids are strongly discouraged for future works due to serious drawbacks like corrosion, toxicity, high energy demand, and the negative environmental impact (Liu et al. 2020).

3.2 Green methods

Environmental issues related to acid hydrolysis using strong acids lead to the development of green methods. Although organic acid hydrolysis and oxidation using ammonium persulfate (APS) are more sustainable options compared to strong acids because they use less polluting solvents, they still damage the environment by producing acid residue in the process. Other more eco-friendly approaches are acid-free preparation methods such as subcritical and supercritical water hydrolysis, enzymatic hydrolysis, mechanical disintegration, and TEMPO-mediated oxidation (Chen et al. 2012; Novo et al. 2016; Zhou et al. 2018).

Organic acid hydrolysis has been studied as a sustainable preparation method for CNCs production since they are easier to recover. The citric acid (Liu et al. 2020), maleic acid (Seta et al. 2020), and formic acid (Du et al. 2016) hydrolysis have been performed to prepare CNCs with thermal stability and high yield. Nevertheless, prolonged reaction times and high acid concentration are required to isolate CNCs with these weak acids.

The oxidative method using ammonium persulfate (APS) is a promising method to isolate CNCs because it dispenses the pretreatment steps to remove lignin and hemicellulose contents of lignocellulosic sources (Zhang et al. 2016). Generally, the method uses a solution with APS molar concentration ranging from 1 to 2 M, time reaction between 14 and 16 h at 60 °C or 70 °C (Leung et al. 2011). These conditions are tunable according to cellulosic raw materials to achieve a higher yield. APS dissolution in water leads to the release of sulfuric acid and oxygen peroxide. Thus, this method uses two mechanisms to break down the disordered regions of the cellulose chain and liberate the crystal structure: acid hydrolysis and oxidation (Fig. 2) (Mascheroni et al. 2016). Nonetheless, the low yield and the prolonged reaction time are two main limitations associated with the APS method.

Subcritical and supercritical water is a green alternative for CNCs production since it uses water as a solvent. This method can cleavage cellulose glycosidic bonds because the water dielectric constant declines at high pressure and temperature, increasing the concentration of H_3O^+ in the medium (Fig. 2C). (Adschiri et al. 2011). Novo et al. (2015) studied CNC's properties obtained from the subcritical process and evaluated the costs compared to acid hydrolysis. The thermal analysis demonstrated that the onset of temperature degradation was higher to CNCs from subcritical hydrolysis and the cost to produce them was lower than acid hydrolysis without considering the purification process. According to further research by Novo et al. (2016), in subcritical water hydrolysis, the degree of crystallinity, length and aspect ratio are mostly influenced by temperature, while yields of CNCs is mainly affected by pressure. Despite the aforementioned advantages of subcritical hydrolysis, it requires a reactor under high pressure and temperature, representing a limitation and high energy costs.

Enzymatic hydrolysis is an environmentally friendly method to isolate CNCs as it does not consume either chemical solvents or high energy levels. This method uses enzymes named cellulases to attack cellulose glycosidic bonds and convert amorph chains into reducing sugars (Chen et al. 2012). Cellulases are mostly produced by fungi, and they are comprised of endoglucanases (able to hydrolyze internal amorph chains), exoglucanases (act at the nonreducing end of cellulose chain) and β-glycosidases (release free sugars from cellobiose repeated unit) (Fig. 2d). (Brandes et al. 2020). The yield of CNCs prepared by the enzymatic method depends on cellulases concentration, reaction time and temperature. For example, Chen et al. (2012) obtained rod-like NCCs from cotton fibers with the highest yield of 32.4% at low temperature, low concentration of cellulase after two days of enzymatic reaction.

Although enzymatic hydrolysis is a green and low-cost method to isolate CNCs, it still suffers from some shortcomings, including the requirement of a long time to convert high solid loadings and the necessity of pre- and post-purification processes (Pereira and Arantes 2020).

Mechanical treatments, such as high-pressure homogenization, ball milling, and ultrasonication (Teo and Wahab 2020), use shearing forces to break cellulose microfibrillar structure and liberate nanoscale particles (Fig. 2e). These techniques are considered a sustainable pathway because they do not use chemical materials (Nge et al. 2013). However, generally, the high content of amorph regions remains after mechanical disintegration; thus, a combination with chemical treatments is necessary to isolate CNCs.

4 Oxidation treatment of cellulose

Cellulose is a high molecular weight linear homopolymer composed of several linkages of 1,4-anydro-D-glucose units that are found twisted 180° with respect to its neighbours (AI-Jawhari 2020). The repeating unit consists of two anhydroglucose rings with polymerization degree range from 10,000 to 15,000 depending on cellulose raw material (Moon et al. 2011). The hydrogen bonds between the hydroxyl groups and the oxygen of the nearby molecules promote a strong intra and intermolecular interaction of the cellulose chains and lead to an arrangement in stacks of structures packed in microfibrils (Moon et al. 2011; Gopi et al. 2019). Due to the lack of chemical or enzymatic process, the microfibrils of native cellulose cannot be disintegrated into monomers in the human body; therefore, it has to be chemically modified to be applied as a biomaterial (Wang et al. 2016). Oxidized cellulose is one of the most used cellulose derivatives for wound dressing because of its high capacity to promote coagulation by contact activation (Yuan et al. 2020). Additionally, this surface modification has improved biodegradability and hemostatic effect compared to the native cellulose (Sezer et al. 2019).

The oxidation process consists of introducing anionic functional groups (carboxyl and aldehyde groups) on the surface of the cellulose chains to few or more of the following purposes: (a) to promote the defibrillation of the microfibril structure and to facilitate the isolation process of the nanoparticles; (b) to decrease the hydrophilicity, and to make the material more compatible with hydrophobic matrices; (c) to develop cellulose derivatives with greater biodegradability and antibacterial activity (Khalil et al. 2014; Tavakolian et al. 2020). In addition, the reaction involves the conversion of alcoholic groups into carboxyl groups without changing the polymeric structure, as it occurs through covalent bonds on the cellulose surface (Luz et al. 2020; Cao et al. 2012).

TEMPO-mediated catalytic oxidation is one of the main methods to modify cellulose microfibrils surface as it promotes selectively oxidation of hydroxyl groups in carbon 6 of the anhydroglucose rings (Cao et al. 2012; Sbiai et al. 2011). This method has already been applied in different cellulose sources such as lignocellulosic fibers: cotton linters (Saito et al. , 2005, 2006), kraft cellulose (Sezer et al. 2019), and bacterial cellulose (Yuan et al. 2020). This type of oxidation consists of adding NaClO as the primary oxidizing agent in aqueous cellulose suspensions in the presence of catalytic amounts of tetramethyl-1-piperidinyloxy (TEMPO) and NaBr under a pH range of around 10–11 and ambient temperature (Fig. 3) (Missoum et al. 2013; Khalil et al. 2014).

The biodegradation, bioabsorbable, bactericidal effect and physicochemical properties of oxidized cellulose are intrinsically related to the oxidation level and can be tailored with the percentage of carboxyl groups introduced in cellulose chains (Zhang et al. 2020). For TEMPO-mediated catalytic oxidation, the oxidation level depends on the oxidant agent concentration, time reaction and the type of cellulose used.

The oxidation level can be determined by different methods such as conductimetry, solid-state nuclear magnetic resonance (NMR), methylene blue adsorption, quantitative infrared and carbazole chemical method. da Perez et al. (2003) reported that methylene blue adsorption underestimates the carboxyl content because the insoluble fraction of cellulose is partially solubilized during the method. The same limitation has been found in the carbazole chemical method because it requires the complete hydrolysis of cellulose monosaccharides to determine the carboxyl content precisely. Therefore, this work was focused on the conductimetric, NMR and quantitative infrared methods, among others.

The conductimetric method uses conductivity variation with ions concentration in a solution to estimate the percentage of carboxyl groups per gram of cellulose. In a typical experiment, a sample of oxidized cellulose is dispersed in a dilute solution of a strong acid to convert all sodium carboxylate groups introduced during the oxidation into protonated carboxyl groups (Zhou et al. 2018). After that, the suspension is titrated with a dilute solution of a strong basic to neutralize the excess acid. Finally, the conductimetric titration curve presents the volume of strong basic solution related to the strong acid added and a volume equivalent to the weak acid corresponding to carboxyl content in the sample (da Perez et al. 2003).

Solid-state nuclear magnetic resonance (NMR) provides the spectra of cellulose oxidized samples where the signals are assigned to the carbons present in the anydroglucose units. The regioselective TEMPO-mediated oxidation is observed by the decrease in the intensity of the signal

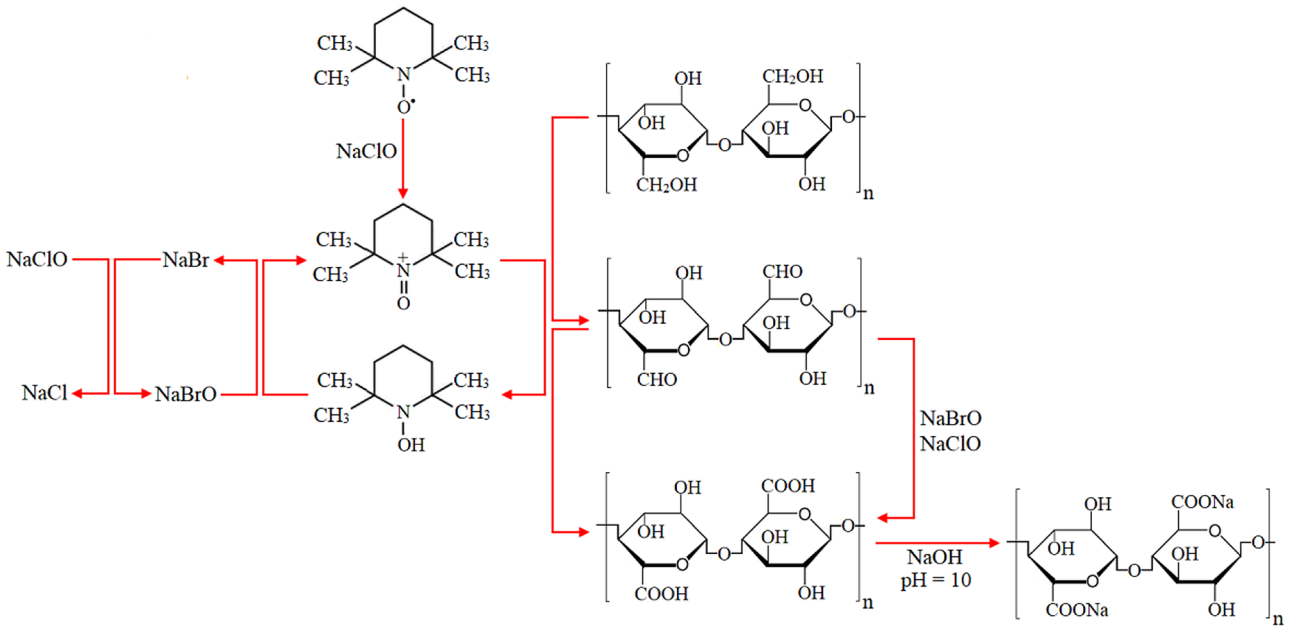

Fig. 3 Schematic representation of the TEMPO-mediated oxidation of cellulose units

corresponding to carbons of primary hydroxyl groups (C6) and the appearance of the signal at around 173 and 175 ppm corresponding to the carboxyl groups (Rohaizu and Wanrosli 2017; Montanari et al. 2005). Thus, the integration of the signal corresponding to the carboxyl groups allows finding the oxidation level of the sample (Montanari et al. 2005).

Infrared spectroscopy can be used to determine the carboxylate content of oxidized cellulose samples. According to da Perez et al. (2003), the most significant change in the spectra of cellulose regarding oxidized cellulose is the appearance of the C=O stretching band at 1608 cm^{-1} or 1730 cm^{-1}, related to carboxylate and acid groups, respectively. The same authors quantified the carboxylate content by acquiring spectra of non-oxidized cellulose and totally oxidized cellulose. They used the same amount of samples in all tests and normalized the curves, considering 0% oxidation level as cellulose spectra area and 100% as totally oxidized cellulose spectra area. Thus, the oxidation level of partially oxidized samples was found by interpolation.

Isogai et al. (2011) verified the influence of NaClO amount used as a primary oxidant agent in TEMPO/NaBr/NaClO oxidation of bleached softwood pulp under pH condition of 10.5 at room temperature. The experiments demonstrated that carboxylate content increases with NaClO added initially, while small amounts of aldehyde were found in the oxidized cellulose. However, the oxidation with NaClO in the range 5 to 10 mM/g reduced the degree of cellulose polymerization to a half.

Saito et al. (2005) studied the influence of time reaction on the oxidation of C6 primary hydroxyls of cellulose by TEMPO-mediated oxidation using cotton linters as raw material at a constant amount of NaClO of 4.84 mM/g cellulose. The degree of oxidation for the oxidation times of 0.5, 2 and 24 h were found to be 7, 13 and 15%, respectively, which indicates that the oxidation level of cellulose increases with the reaction time. This study also revealed that carboxylate and aldehyde groups were introduced just on the surfaces of cellulose I crystallites; in other words, these structures were not affected by oxidation reaction. Khalil et al. (2014) explained that the initial materials significantly influence the nature of the resultant material of TEMPO-mediate oxidation. When native cellulose (identified as cellulose type I) is used, even under harsh conditions, oxidation happens only at the surfaces of the crystals.

In their subsequent work, Saito et al. (2006) investigated TEMPO-mediated oxidation using cotton linters, ramie, and spruce holocellulose as raw materials using 2.42 mM/g of NaClO. The results showed that oxidation efficiency is related to the crystal size of the native crystalline structure of cellulose I. Therefore, the efficiency of the treatment increases from cotton linters, which possesses a crystal size of 6.2 nm, to spruce holocellulose that have 3.2 nm of crystal size. Furthermore, the study revealed that neither carboxylate nor aldehyde groups are formed inside the crystal structure.

In a more recent study, Sezer et al. (2019) studied the hemostatic activity, degradation, and the bactericidal effect of two types of OC and ORC. Hutchinson et al. (2013) defined ORC as a material prepared through a chemical process that uses native cellulose as the initial material. Thus,

ORC has a lower molecular weight, a lower degree of crystallinity and a more uniform fiber diameter, which leads to more uniform and consistent oxidation.

In a first analysis, Sezer et al. (2019) found that OC and ORC had different degrees of oxidation for the same conditions and assumed that this could be correlated to the differences between the amorphous and crystalline regions of the raw materials. At the same time, an increasing trend was found in the degree of oxidation with the reaction time. In the hemolysis assay, the authors found that the hemostatic rates increase with the degree of oxidation for the two types of oxidized cellulose studied. However, in terms of degradation, the OC showed better results, mainly with the increase in its degree of oxidation. Therefore, they concluded that the two aspects must be considered when choosing the cellulose-based material: the degree of oxidation and type of cellulose.

TEMPO-mediated oxidation is also used to isolate cellulose nanocrystals, named TEMPO-oxidized cellulose nanocrystals (TOCNCs). Relevant analyses have demonstrated the improvements in morphological, mechanical and swelling properties when this nanoparticle is incorporated on a polysaccharide matrix (Deepa et al. 2020). Therefore, the oxidation treatment of cellulose nanocrystals may be an appropriate option to achieve the required properties for wound dressing applications.

5 Mechanism of hemostasis

Wound healing is a highly coordinated spatiotemporal regulator that consists of multiple cellular and molecular events and involves four highly integrated stages, as described in Fig. 4: Hemostasis, inflammation, proliferation, and remodelling (Fazil and Nikhat 2020; Kordestani 2019; Moeini et al. 2020; Oyama et al. 2020; Xiang et al. 2020).

After suffering a trauma (wound), there is a break in the integrity of the tissue, which causes damage to the blood vessels and the activation of the coagulation cascade. This first stage of the healing process is called hemostasis and occurs immediately after the injury to stop bleeding (Fazil and Nikhat 2020; Kordestani 2019).

Hemostasis happens in three fast and coordinated stages and mainly involves platelets and proteins responsible for coagulation and fibrinolysis. The first stage, known as vascular spasm or vasoconstriction primary hemostasis, is a response of the organism immediately after the trauma. Vasoconstriction of the injured vessel manifests itself to decrease local blood flow and, thus, prevent hemorrhage or thrombosis. When the second stage initiates, the free platelets present in blood flow are activated and adhere to the endothelium of the injured vessel using a glycoprotein known as von Willebrand factor, which helps to stabilize more platelets to the lesion site, forming a physical barrier for the entry of pathogens (Fazil and Nikhat 2020; Kordestani 2019). Finally, in the following third stage of hemostasis, a complex repair of the injury occurs by the coagulation cascade with the activation of proteins responsible for coagulation, and fibrinogen transformation into fibrin that reinforces the primary platelet plug and, thus, stops bleeding (Fazil and Nikhat 2020; Kordestani 2019). The Fibrin network acts as a barrier against microorganisms and forms a temporary matrix essential to cell migration. Fibrin temporary matrix preserves tissue integrity, an essential factor in wound healing (Gonzalez et al. 2016).

The next stage of healing is the inflammatory reaction, which begins simultaneously with the initial healing process, characterized by the main signs of inflammation, such as edema, pain, and swelling (Fazil and Nikhat 2020). This phase involves several immune system cells, molecular mediators, and blood vessels (Fazil and Nikhat 2020; Xiang et al. 2020). The first 24 h are dominated mainly by the

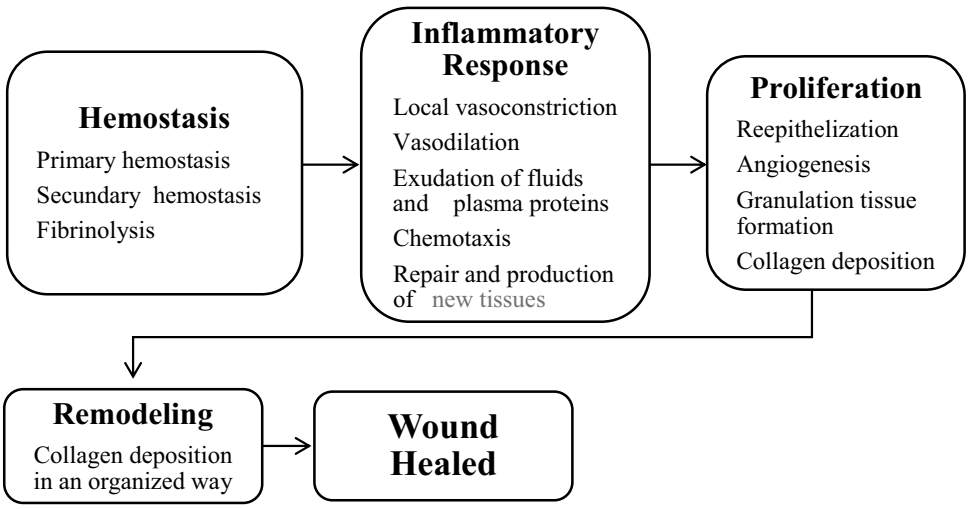

Fig. 4 Main stages of the wound healing process

action of neutrophils, leukocytes, and lysosomes responsible for phagocytosing debris and pathogens, releasing proteolytic enzymes, chemokines, and cytokines at the injury site induce tissue repair and fibrin degradation (Fazil and Nikhat 2020; Kordestani 2019). During the early 72 h as this process occurs, degradation products attract fibroblasts, and epithelial cells and blood monocytes release tissue macrophages. These macrophages, along with phagocytosis of debris, release biological regulators, growth factors such as TGF-β, MCP-1, and proteolytic enzymes that promote the development of new tissues by stimulating fibroblasts keratinocytes, and angiogenesis (Fazil and Nikhat 2020; Kordestani 2019; Moeini et al. 2020).

The third stage of the healing mechanism is the proliferation, characterized by the gradual closure of the wound through the migration of keratinocytes, collagen formation, revascularization, regeneration of epithelial tissue, and epidermis restoration, making it again continuous and functional. (Fazil and Nikhat 2020; Kordestani 2019; Moeini et al. 2020). This phase is dominated by the action of fibroblasts, leukocytes, pericytes, and endothelial cells and lasts from 3 to 21 days after the injury (Fazil and Nikhat 2020; Kordestani 2019).

Finally, the remodelling of the injury site, as the last healing step, can take, depending on the case, 2–3 weeks or more than a year, and it is responsible for the increase in tensile strength, the contraction of the wound, and the decrease in the scar (Fazil and Nikhat 2020; Kordestani 2019). This process is characterized by changes in the composition of the extracellular matrix and the replacement of type III to type I collagen so that the newly synthesized collagen fibers are crosslinked and organized along the tension lines (Kordestani 2019; Moeini et al. 2020). It is worth mentioning that even after one year, the wound will still have less organized collagen, and the tensile strength of the scar tissue will reach around 80% but never return to 100% (Kordestani 2019).

5.1 The role of cellulose in the mechanism of hemostasis

As previously discussed, the hemostasis process is the first stage of wound healing. The success of this stage is essential to prevent severe hemorrhage that could even lead the patient to death during or after surgical intervention. A strategy to provide rapid hemostasis in emergencies is using hemostatic agents, as polysaccharides (chitosan, alginate, collagen, starch, others), which have stood out in recent years (Yang et al. 2017; Zhang et al. 2020). Natural polymers derived from cellulose have shown interesting properties in hemostasis in the long term, but the comprehension of their hemostasis mechanism remains unclear and needs further investigations (Cheng et al. 2016b; Yang et al. 2017; Zhang et al. 2020).

Before discussing the hemostatic mechanisms of cellulose, it is worth mentioning that an excellent hemostatic agent must have rapid hemostasis, high biocompatibility, non-cytotoxicity, good biodegradability, high capacity to stimulate the healing process, low cost, and easy processing (Yang et al. 2017; Zhang et al. 2020).

The mechanisms of hemostasis are activated when suffering an injury and will depend on many factors, such as the types of hemorrhages and the properties of the material. The mechanism can be performed by activating the coagulation cascade or blocking the bleeding site (Yang et al. 2017; Zhang et al. 2020). Cellulose, in particular, stands out more in this last-mentioned route, also called the passive route (Yang et al. 2017). The latest studies show that materials based on oxidized cellulose, especially hydrogels and foams, can quickly absorb most of the liquid in the blood, increasing the concentration of blood clotting factors and accelerating the formation of a fibrin clot (Cheng et al. 2013; Yang et al. 2017; Zhang et al. 2020) (Fig. 5). This process is independent of the coagulation cascade.

Another phenomenon is the onset of coagulation via autoactivation of coagulation factor XII by the negative net charge on the cellulose surface due to carboxylate anions. (Cheng et al. 2016b, 2013; Yang et al. 2017). In addition, low pH conditions related to carboxyl groups causes non-specific platelet aggregation due to the strong complexing capacity of the Fe^{++} with Hemoglobin, thus promoting the formation of an artificial clot (Cheng et al. 2013; Martina et al. 2009). However, this low pH limits applications to sensitive tissues, such as tissues of the nervous and cardiac systems, as well as causing an increase in the cytotoxicity of the material (Ohta et al. 2015; Wu et al. 2018b). Figure 5 presents a scheme of one of the possible mechanisms for hemostasis using the ORC device.

Another important point highlighted by Cheng et al. (Cheng et al. 2016a) is that ORC with larger microscopic dimensions (> 80 µm) decreases the absorption of blood fluids, which limits its application, being used only in minor wounds with less intense bleeding. This fact shows the need to manufacture materials with larger contact areas, such as dressings obtained on the nanometric scale, ensuring greater fluid absorption efficiency.

Cheng et al. (2016a) proposed an oxidized microcrystalline cellulose (OMCC) dressing. The authors evaluated the homeostatic effect of OMCC and compared the results with a traditional gauze with oxidized regenerated cellulose (ORC) and the ORC/OMCC composite. The cell viability results showed that in the first 24 h, ORC showed a decrease in cell proliferation, while OMCC and the ORC/OMCC composite increased cell proliferation. On the other hand, after 48 h, there was a similar increase in cell proliferation in all tested materials (Fig. 6a). In vivo biodegradation tests showed that with two weeks of testing,

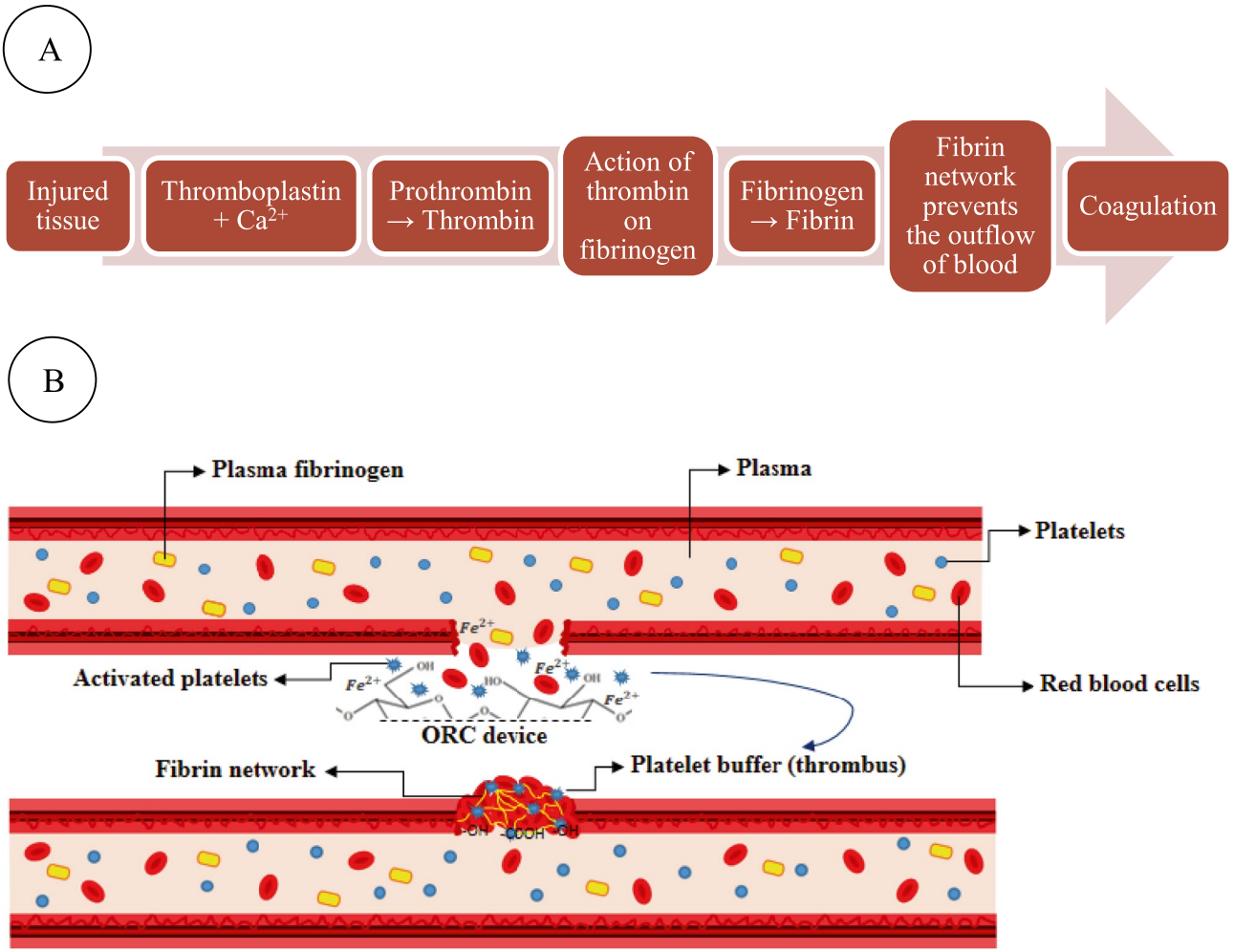

Fig. 5 Scheme of one of the possible mechanisms of hemostasis using ORC device. **A** The sequence of steps that occur during the blood clotting process. **B** Blood vessel wall rupture, platelet adsorption and activation, and thrombus formation

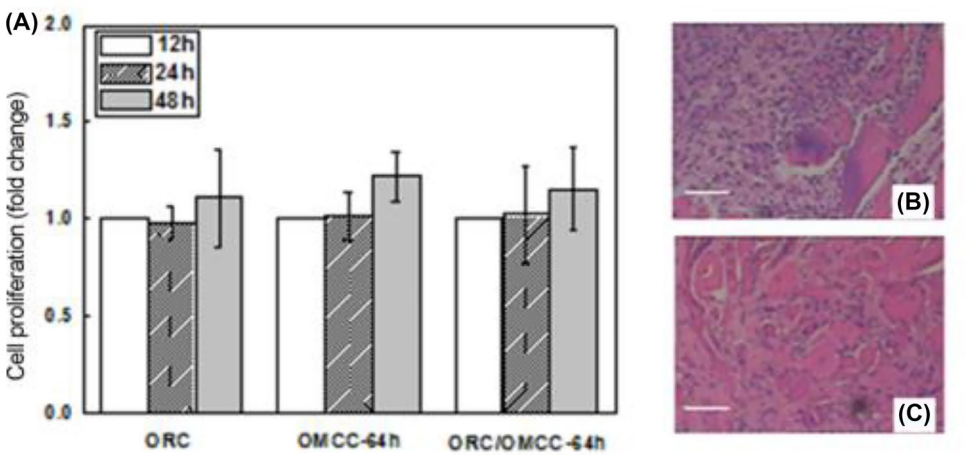

Fig. 6 Cell proliferation (**A**) on TCPs cultured for 12 h, 24 h and 48 h in DMEM with different material extracting solutions (material/ PBS, 1 g/1 ml, w/v). Photomicrographs of ORC-OMCC-64 h composite on subcutaneous implantation site for 2 weeks (**B**) and 4 weeks (**C**). The scar bar is 100 μm. Reproduced with permission from Ref. (Cheng et al. 2016a). Copyright 2016, Springer Nature

there were still remnants of the ORC/OMCC compound at the implanted site (Fig. 6b), and complete degradation occurred only within four weeks (Fig. 6c).

The authors also showed that the ORC/OMCC composite exhibited prominent hemostatic property in the aspect of shorter average hemostatic time and less blood loss when compared with ORC and OMCC alone and with gauze. The study was conducted in two models: The middle ear artery model and the liver trauma model. In the rabbit liver injury model, the hemostatic time of three materials (ORC, 257 ± 33 s; OMCC-64 h, 176 ± 42 s and ORC/OMCC-64 h composite, 173 ± 22 s) were significantly less than the Gauze group (> 600 s). In the rabbit ear artery injury model, the hemostatic speed of the ORC/OMCC64 h composite (131 ± 42 s) was faster than the ORC (178 ± 48 s), OMCC-64 h (151 ± 32 s), and gauze (> 600 s). The difference was statistically significant as $p < 0.05$ (Cheng et al. 2016a).

Finally, the authors evaluated the clotting process in vitro by determining small changes in the concentrations of different blood clotting factors by ELISA. The results, shown in Fig. 7, indicate that the progress of hemostasis occurred from intrinsic coagulation; that is, all the components necessary for the clotting process to proceed are found in the blood, and the activation of factor XII initiated the coagulation process. Thus, the authors concluded that the hemostasis mechanism of the ORC/OMCC composite is a combination of physical adsorption and physiological hemostasis (Cheng et al. 2016a).

Liu et al. (2018) created a green nanocomposite hydrogel by introducing aminated silver nanoparticles (Ag-NH2 NPs) and gelatin (G) in carboxylated cellulose nanofibers

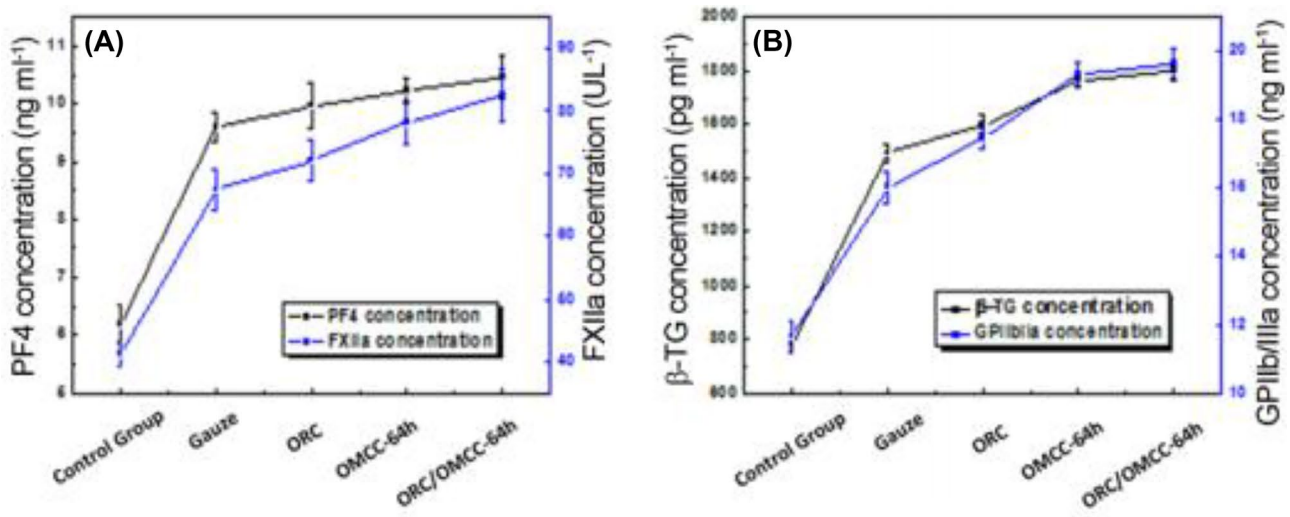

Fig. 7 The Effecting trend of different samples to the various factors. The release of PF4 (**A**) and β-TG (**B**) are enhanced just after platelets are activated. Factor FXIIa (**A**) increase plays a vital role to start the intrinsic coagulation pathway. The concentration of GP IIb/IIIa (**B**) increases when the activated platelets aggregate. Reproduced with permission from Ref. (Cheng et al. 2016a). Copyright 2016, Springer Nature

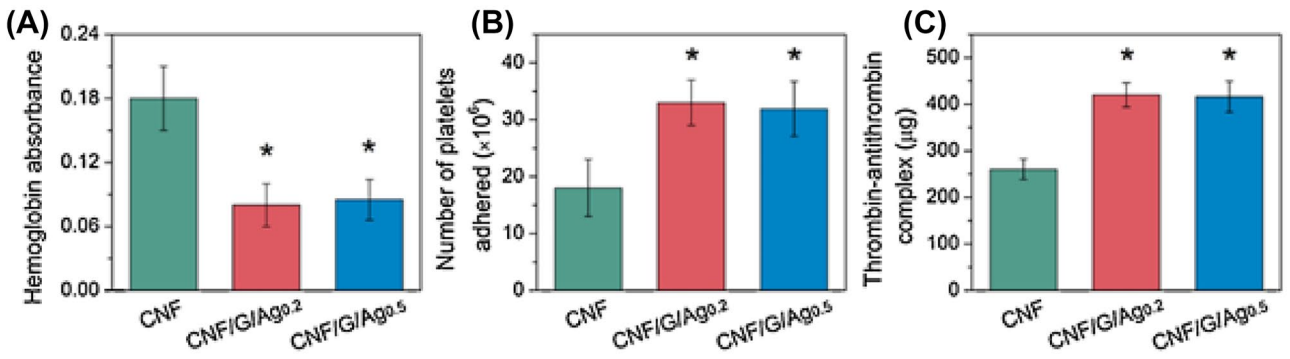

Fig. 8 The blood clotting results as measured by (**A**) absorbance of haemoglobin, (**B**) platelet adhesion, and (**C**) thrombin generation as evaluated from thrombin–antithrombin complex. Reproduced with permission from Ref. (Liu et al. 2018). Copyright 2018, Elsevier

(CNF). The results, which are shown in Fig. 8, showed that the CNF/G/Ag interpenetrating network had higher blood-clotting capacity (Fig. 8a), more platelets (Fig. 8b), and thrombin-antithrombin complex (Fig. 8c), which shows that the multi-component structure benefited the hemostatic properties.

The in vivo tests showed that the treatment of the wounds of mice with CNF/G/Ag was highly favourable and that the results were especially favoured by the synergy between the components of the formulation (Fig. 9).

Cheng et al. (Cheng et al. 2017) prepared oxidized cellulose nanocrystals (TONC)/alginate (SA) composite films and sponges with different weight proportions. The results showed that the blood loss of sponges for both the rabbit liver injury model and the ear artery injury model was lower than that of films (Fig. 10).

In general, the hemostatic effect of the TOCN-30/SA composite sponge was better than the TOCN-30/SA film due to its excellent hemostatic properties, such as blood loss and hemostatic time. The authors suggest that these results are related to the porous structure presented by this material, which was beneficial for quickly absorbing the blood on its surface with great capacity, that made it more conducive to promote the aggregation of platelets and induce erythrocytes to accelerate the clotting of the blood (Cheng et al. 2017).

Few clinical studies in the literature have demonstrated the efficacy and safety of ORC as a hemostatic agent. Masci et al. (2018) made a retrospective analysis of data from patients undergoing laparoscopic cholecystectomy in the Division of General Surgery, Hospital Edoardo Bassini, Cinisello Balsamo, Italy, between October 2014 and February 2016. In the 16 months, 530 patients underwent laparoscopic cholecystectomy. The use of ORC gauze during surgery was required in 24 (4.5%) patients [10 males and 14 females, median age 58 years (range 18–84)], as conventional methods (monopolar or bipolar electrocautery) failed to adequately control bleeding from the liver bed who underwent laparoscopic cholecystectomy. The authors' main objective was to describe the use and results of topical hemostasis with ORC in patients with difficult-to-treat

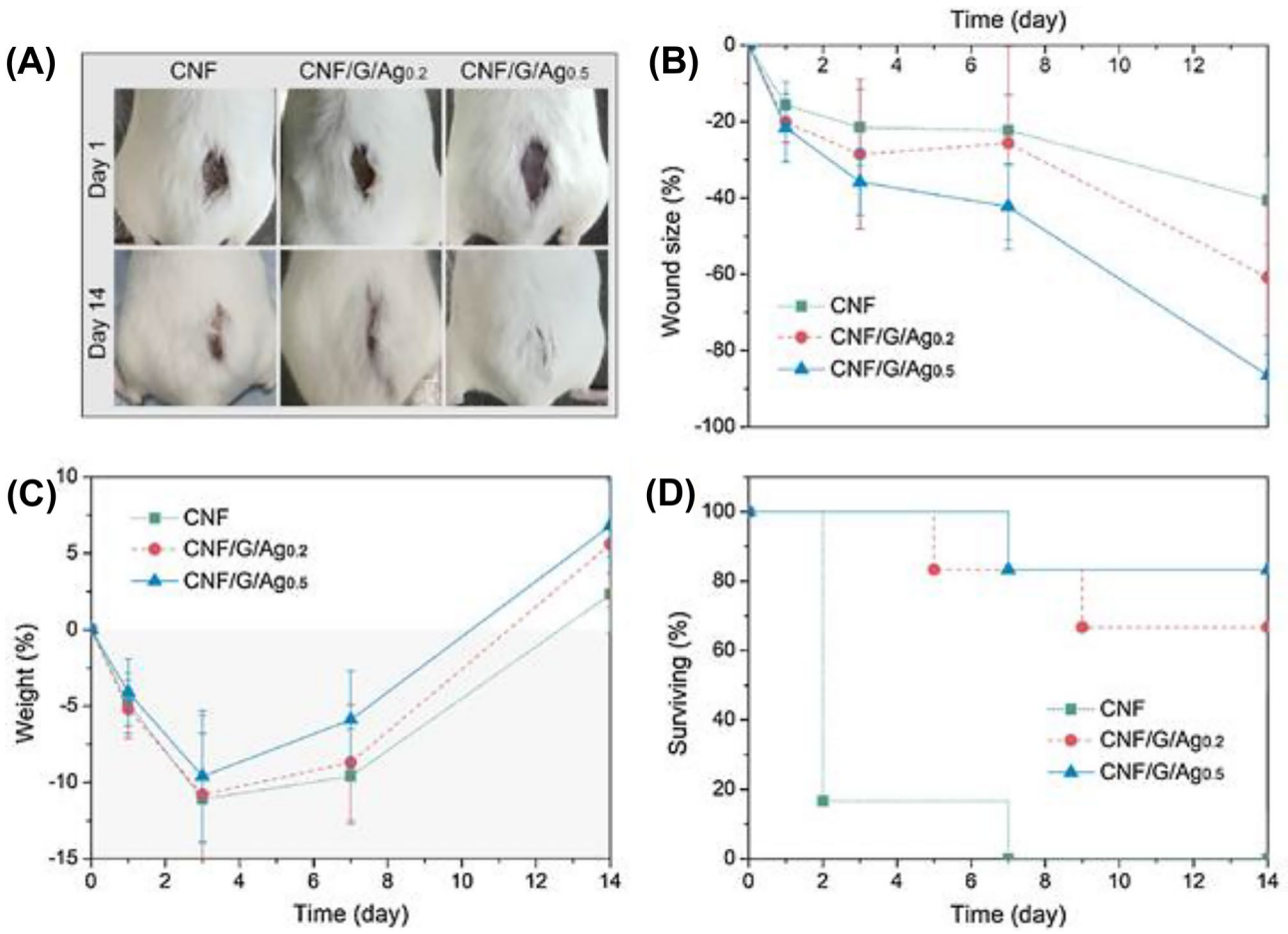

Fig. 9 Mice by different dressing treatment: (**A**) photographs, (**B**) wound size change, (**C**) weight change, and (**D**) survival. Reproduced with permission from Ref. (Liu et al. 2018). Copyright 2018, Elsevier

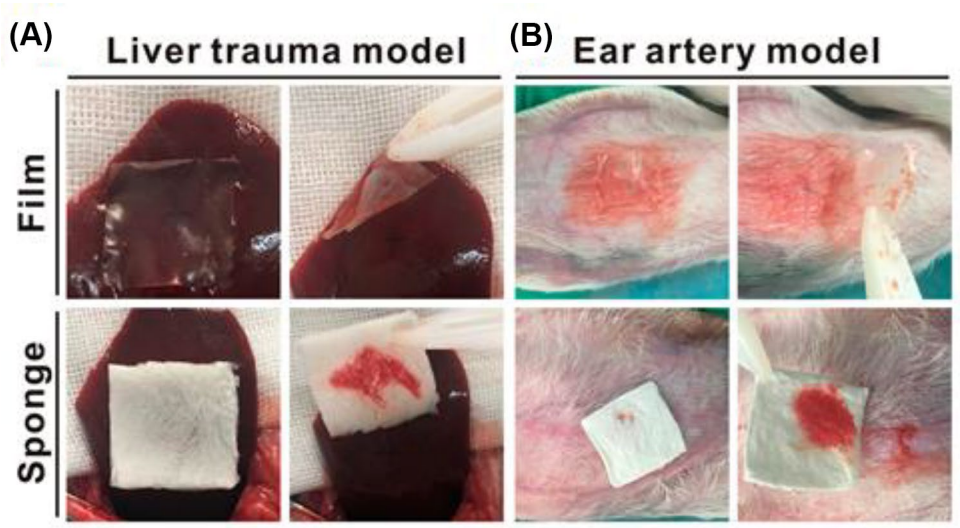

Fig. 10 Hemostatic effect of neat SA, TOCN/SA composite films, and TOCN/SA composite sponges on the different trauma of the rabbit: (**A**) the liver and (**B**) the ear artery. Adapted with permission from Ref. (Cheng et al. 2017). Copyright 2017, ACS Publications

bleeding during laparoscopic cholecystectomy. Difficult-to-treat bleeding was assessed based on the flow and depth of bleeding during laparoscopic cholecystectomy. If bleeding continued uncontrolled for a few minutes despite conventional hemostatic techniques, ORC gauze was applied to the liver bed to avoid prolonged use of electrocautery to prevent damage to the parenchymal tissue. The results were excellent compared to conventional methods that were not efficient in this case. The authors found that a disadvantage of using ORC is its potential to swell, which causes pressure on adjacent tissues and organs; so, ORC removal is required after the surgery close to the sensitive areas. Despite this, the study highlighted the great potential of its applicability and opened new doors for more investigations for improving the material by controlling its swelling degree.

Another interesting case study was presented by Capozza et al. (2016), in which a 54-year-old male patient, previously operated for meningioma (grade II) using Surgicel™ (ORC) to prevent bleeding in the surgical site, complained of weakness in his left arm one month after surgery. After imaging exams (computed tomography and magnetic resonance), it was shown granulomatous reaction by a foreign body, which rarely occurs in practice.

Both clinical studies presented here exhibit the need for further studies and show that the patient's demographic and clinical characteristics are fundamental for the application of ORC.

6 Nanocomposites with CNCs for wound healing

Nanocomposites are classified as a class of materials composed of a disperse phase, named matrix, and a reinforcing phase with particles in nanometric scale, 1–100 nm. The advantage of using nanocomposites is their capacity to improve and bring together the properties of different components by incorporating structures with small sizes. Cellulose nanocrystals (CNCs) have been extensively studied as reinforcing material due to their outstanding mechanical properties, availability for chemical modification, high contact surface, and renewability. Furthermore, combining CNCs with other biopolymers leads to the fabrication of nanocomposites for wound healing applications, improving their physical and biological properties. This section presents the most common biopolymers used as a matrix for CNCs nanocomposites and their preparation to be applied as wound healing.

6.1 Chitosan

Chitosan (CS) is a polysaccharide formed by the deacetylation of chitin, one of the most abundant natural polysaccharides on earth (Dai et al. 2011). Chitosan has a polymorphic crystalline structure, and it is composed of very reactive molecules with an amino-functional group and two hydroxyl groups, which allows the modification of the surface and the excellent interaction with other molecules (Archana et al. 2016).

Positively charged chitosan has intrinsic antimicrobial properties against gram-positive and gram-negative bacteria types and fungi. This fact is attributed to the interaction of ammonium groups of CS with the negatively charged surface of the microbial cell membranes (Dai et al. 2011; Archana et al. 2016). Additionally, CS has hemostatic and biocompatible properties and improving properties because CS decomposition leads to fibroblast proliferation and orderly collagen deposition (Ostadhossein et al. 2015).

Naseri et al. (2015) made a bionanocomposite with Chitosan/Polyethylene Oxide (PEO) blend as a matrix

phase and cellulose nanocrystals as the reinforcing agent and studied its properties for wound dressing application. Porous fibers mats of CS/PEO/CNC were obtained through electrospinning technique, and the analysis of its mechanical properties revealed that the inclusion of CNCs, in the matrix phase led to an improvement in the tensile strength. This characteristic behaviour is important since dressing materials are supposed to be soft and flexible to bear the stress caused by some parts of the body. Furthermore, permeability tests with CS/PEO/CNC mats demonstrated that the introduction of CNCs has two opposite impacts on wound healing rate. On one side, it increases the permeability of O_2 and water vapour, facilitating the wound healing process by allowing collagen synthesis and angiogenesis and preventing the cell from dying for dehydration. On the other side, it increases the CO_2 diffusivity that hinders the healing rate. Moreover, in vitro analysis showed that fiber mats bionanocomposites did not present any cytotoxicity or inhibition zone of cell growth after seven days, making them a favourable biocompatible material for wound dressing.

A study made by Poonguzhali et al. (2018) verified the properties of a bionanocomposite of Chitosan/PVP/nanocellulose as a candidate for wound dressing applications. The mechanical tests of the thin and porous material revealed that the elongation at break with 3% of CNCs in the matrix was higher than the nanocomposite with 5% of CNCs. This result was because the motion of the CNCs in the polymer matrix chains at higher concentrations was limited. As for wound dressing materials, flexibility is essential to cover the wound surface adequately; the composite with 3% CNCs presented better mechanical properties for this application.

The swelling analysis of Poonguzhali et al. (2018) showed that the incorporation of nanocellulose increased the swelling capacity of the matrix as a result of the interaction between the hydroxyl groups of the water and hydroxyl and carboxyl groups of the cellulose molecules. This result is clear evidence of the better capacity of this material to absorb the exudates from the wound.

Other results from Poonguzhali et al. (2018) were found in the biological properties of the bionanocomposities when CNCs were introduced in the CS/PVP matrix. It was verified better antibacterial responses for both gram-positive and gram-negative bacteria for composites containing 3% and 5% of CNCs. The in vivo wound healing tests, carried out using Albino rats, revealed superior wound healing efficiency for the CS/PVP membranes and bionanocomposite with 3% of CNCs, compared to the control (Povidoneiodine ointment). In addition, CS/PVP/CNC 3% provided a completely wound restoration after 21 days, while the control and CS/PVP membrane presented a low healing rate.

6.2 Collagen

Collagen (COL) is a fibrous structured protein found in the extracellular matrix of diverse animals such as bovine, equine, porcine, frog, bird, and some of marine origin as catfish, marine sponge, squid, redfish, etc. (Albu et al. 2011). It is the principal constituent of connective tissues such as skin, tendons, ligaments, cartilage, cornea, and bones. In addition, it plays a structural hole in vertebral bodies (Rodrigues et al. 2017).

Collagen is constructed by polypeptides containing triamino acid blocks formed into triple helix microfibrils that can assemble in different arrangements to supply different functions (Ulery et al., 2011).

The use of COL in the biomedical application is recognized for its remarkable biological properties such as biocompatibility, low toxicity, cell adaptability, high structural support for tissue regeneration and controlled biodegradability (Rodrigues et al. 2017; Cheng et al. 2016b). Moreover, this biomaterial has been the subject of studies for its efficient use as a hemostatic sealant in wound healing applications because it promotes the natural clotting formation by activating fibrogen conversion into fibrin and because it coats the wound surface properly (Ulery et al. 2011).

Slezak et al. (2018) compared the mechanical properties, swelling capacity and in vivo adhesion formation of collagen-based hemostatic (PCC) patch and oxidized cellulose-based patch (PCOC). The study demonstrated better mechanical stability for PCC, after two h of incubation in human plasma, and a loss of the mechanical properties by PCOC due to the faster degradation of the cellulose molecules than collagen, by phagocytosis process in which foreign substances are ingested by specific cells as a defence mechanism. Furthermore, the swelling test showed that although the PCOC has greater swelling capacity than the PCC, its volume and thickness increased significantly, which may limit its use in confined spaces. Moreover, the PCC showed less formation of adhesions in vivo than the PCOC, which means that PCC may offer fewer postoperative complications.

In another study, Cheng et al. (2016b) prepared ultra porous collagen/ORC hemostatic composites in a sponge form and verified physical properties, biological safety in vitro and hemostatic and biodegradability properties when applied in vivo. Contents of 0.25, 0.5 and 1% of ORC were added to the collagen matrix and evaluated physical and biological properties. In addition, they checked that the collagen sponge presented higher tensile strength values than the composites. Nonetheless, the composite with 0.25% of ORC presented the highest density of pores and more water absorption capacity, which could be helpful to enhance blood absorption and, consequently, increase the concentration of coagulating agents in the blood. Furthermore,

cytotoxicity tests showed that the composites with ORC mass fractions of 0.25 and 0.5% did not present any toxicity to the cells. However, slight toxicity was observed in the composite with 1% ORC, and it was attributed to a possible increase in the acidic environment by the presence of more carboxyl content.

Moreover, the COL—0.25% ORC composite presented the shortest hemostatic time and the lowest bleeding amount for the two evaluated injury models. Thus, COL—0.25% ORC demonstrated a better capacity to activate blood coagulation factors than the control and COL sponges. Its ultra porous surface, wettability capacity, and hydrophilic carboxyl groups are the main reasons for its good hemostatic performance. Finally, the biological degradation test showed a complete degradation after 28 days for Control material (Trauer collagen without ORC), COL, and COL—0.25% ORC sponges, but pure collagen and COL—0.25% ORC afforded a better tissue restoration.

Composite films containing collagen and cellulose nanocrystals (CNCs) were produced by Li et al. (2014) and evaluated regarding their physical–chemical properties and cell viability. The swelling capacity of the films increased until the concentration of CNCs reached 5%; higher concentrations led to a decline in the swelling ratio. Nevertheless, the nanocrystals were attractive for use as a charge of the collagen matrix because they facilitated the interior ordering and stability of the films and improved the swelling rate. Furthermore, the addition of CNCs in the collagen matrix also improved thermal properties by increasing the degradation temperature from 310 °C for pure collagen film to 350 °C for collagen/CNC composite film with 7 wt% of CNCs. Furthermore, in contrast to the result obtained for the collagen/ORC composites, the mechanical analysis of collagen/CNCs films showed a significant improvement of the mechanical properties, sustaining more stress, especially at high strain levels. Lastly, the cell viability test exhibited a biocompatible behaviour for both collagen and collagen/CNC composite film with 7 wt% of CNCs. All these characteristics envisage the composite films of COL/CNCs appropriate for use as wound dressings.

It is worth noticing that introducing cellulose nanocrystal in the collagen matrix improved mechanical and thermal properties due to its outstanding reinforcing properties and good dispersion without diminishing the biological properties. Thus, CNCs could be a more attractive choice for the reinforcing phase in collagen than ORC.

6.3 Gelatin

Gelatin is a biomaterial derived from collagen through the denaturation process where the well-establish triple helix structure of collagen is separated into individual coil chain structures due to the breaking down of the hydrogen bonds (Djabourov and Papon 1983). As well as collagen, the gelatin has biological properties that make it suitable for biomedical applications such as biocompatibility, biodegradability and non-immunogenicity. Besides, after being solubilized in an aqueous solution, it can be molded in a physically stable gel with the same helix conformation of collagen at temperatures lower than 35 °C and can form a coil structure, like proteins, at higher temperatures, after melting to form a solution (Kuijpers et al. 1999).

Gelatin has gained attention for its use as wound dressings because of its hemostatic properties, capacity to promote cellular attachment and growth and porous structure that absorb wound exudates and maintain a moist environment in the wound (Gaspar-Pintiliescu et al. 2019). However, gelatin does not present desired mechanical properties on its own to be applied as a sealant material in wound healing applications. For this reason, this biomaterial is commonly used with other polymeric additives to improve its performance (Cohen et al. 2014).

Hivechi et al. (2019) investigated the effects of CNCs incorporation into gelatin nanofibers on their morphological, mechanical and biological properties. The nanocomposites were produced by electrospinning technique with different amounts of CNCs (0–15% w/w), and an increase of the viscosity was observed as a function of the CNCs content added in the solution. The statistical evaluation of the tensile strain tests revealed that the mechanical properties were significantly affected by the introduction of CNCs in gelatin nanofibers. An increase in modulus and tensile strength was observed up to the 5% CNCs nanocomposite. Conversely, for higher levels of CNCs, a decrease in these properties was observed. This behaviour was explained by the particle agglomeration of CNCs that created stress regions in the structure of the mat. Besides, the elongation at break decreased with the amount of CNCs introduced into gelatin nanofibers, representing an obstacle since wound dressing material is supposed to have good flexibility. Concerning biological properties, biodegradability measurements during 7, 14, 21, and 28 days were performed, and their results exhibited an improvement of this property with the introduction of CNCs in gelatin nanofibers. While for pure gelatin nanofibers, the weight reduction after 28 days was about 10%, for the nanocomposites with CNCs were reached between 15 and 25% after the same time. The highest weight reduction belonged to the composites with 2.5% and 5% of CNCs. The authors pointed out the high concentration of hydroxyl groups on the surface of CNCs, which can absorb more water and accelerate hydrolysis, as the reason for nanocomposites reaching higher degradation rates. Moreover, the MTT assay, SEM imagens and live/dead cell assay evaluation demonstrated that both pure gelatin mats and nanocomposites with CNCs allowed the

growth and proliferation of cells. No statistical significance was observed about the influence of CNCs addition in the gelatin nanofibers.

In another study, Yin et al. (2019) prepared and characterized 3D porous hydrogels composites using gelatin (GA), hyaluronic acid (HA) and CNCs. According to Graça et al. (2020), HA is a natural macromolecule in the extracellular matrix with high hydrophilicity that could maintain the wound hydrated and perform exudate absorption. The hydrogels were prepared by the freeze-drying method, and micrograph images showed that the introduction of CNCs in both GA and HA matrices provided more circular and uniform pores. As a result, a smooth and porous structure with pore size from 80 to 120 μm, suitable for cell growth, was obtained in the GA-HA composite matrix case. The swelling ratio is an important characteristic to ensure a moist environment at the wound site. Tests presented better results for GA-HA-CNC hydrogel than GA-HA and GA-CNCs composites, and the data also revealed an improvement due to the embed of CNCs in the gelatin and hyaluronic acid matrices separately. Additionally, an enhancing of the hydrogel mechanical properties was observed with the incorporation of CNCs. This nano charge increased the tensile modulus of both pure GA and pure HA hydrogels, and better results were obtained for the GA-HA matrix containing CNCs compared to GA-HA hydrogel.

Moreover, in the same study, the cytotoxicity tests revealed that GA-HA-CNCs hydrogel improved cell metabolism by increasing time culture. The authors detailed that this behaviour could be credited to the good diffusion promoted by hydrophilic gelatin, hyaluronic acid and cellulose matrix that allowed the transport of nutrients from the medium culture. Finally, live/dead analysis showed that after two days of culture, basically no dead cells were found in the GA-HA-CNC hydrogel structure, suggesting that it can supply a survival environment for cells growth and proliferation.

6.4 Alginates

Alginates cover substances derived from alginic acid, characterized as natural anionic polysaccharides extracted from brown algae (Aramwit 2016). At pH above 4, the alginate carboxyl groups can interact with divalent cations, which act as crosslinkers to form stable gel complexes (Agulhon et al. 2012; Rhein-Knudsen et al. 2015; Hatami et al. 2020).

As hydrocolloids, alginate and its derivates have been explored as biomaterials for medical applications such as drug delivery, tissue regeneration and wound healing (Hariyadi and Islam 2020). In addition, some studies demonstrated its capacity to promote angiogenesis, stimulate collagen types formation during the remodelling phase, promote the production of coagulator factors, and its outstanding swelling performances (Wang et al. 2019, 2015; Balakrishnan et al. 2005).

Moreover, other advantages of using alginate are manufacturing dressings that can be easily removed from the wound, causing less pain in the process and the ability to aggregate other biomaterials and bioactive molecules with careful control of their structures (Varaprasad et al. 2020).

The introduction of cellulose nanocrystals in the alginate matrix has been widely studied because of the compatibility of these two biomaterials, which belong to the same polysaccharide family. Also, the three-dimensional structure created by the interaction of alginate and divalent cations, like calcium, provide a good dispersibility of CNCs (Lin et al. 2011). This property helps to avoid the self-aggregation of the nanoparticles and improves the homogeneity of the nanocomposite, which is crucial to its mechanical properties.

A recent study by Deepa et al. (2020) evaluated the introduction of two types of nanocelluloses, cellulose nanofibrils and cellulose nanocrystals, in a sodium alginate matrix. Nanofibrils and nanocrystals were chemically modified with TEMPO oxidation treatment to prepare bionanocomposite films and investigate their effects on structural, morphological and surface properties. The morphological analysis demonstrated that the oxidation treatment produced smoother surfaces compared to non-oxidized types of nanocellulose. Though, a higher tendency of agglomeration was observed in the composite with cellulose nanofibrils. The decrease of roughness indicates the excellent dispersion of nanostructures in the composite matrix. AFM images proved that composites with CNCs presented lower roughness than composites with nanofibrils and that oxidation and ultrasonication processes can induce a better dispersion of nanoparticles in the sodium alginate matrix.

A study by Zhao et al. (2020) showed that incorporating 1% wt CNCs in the calcium crosslinked alginate matrix significantly improved the hydrogel swelling properties. Moreover, the nanocomposite provided a better drug loading capacity and slower release rates. These characteristics can make these composites studied attractive biomaterials for wound dressing and drug delivery applications.

Cheng et al. (2017a) produced two types of dressings, film and sponges, by incorporating different amounts of TEMPO-oxidized cellulose nanocrystals (TOCNCs) in an alginate matrix crosslinked with Ca^{2+} cations. The morphological analysis showed a good interaction between cellulose nanoparticles and alginate with no aggregates, resulting in a homogeneous 3D porous structure. Furthermore, it was found to increase the porosity, compared to pure alginate matrix, from 82% to values above 90% for the composites. As a consequence, the swelling capacity was improved for both materials, films and sponges. Nonetheless, the sponges presented higher swelling ratios than the films due to their large contact surface area and internal network.

The mechanical test revealed that the introduction of TOCNCs enhanced the tensile strength of neat alginate films and sponges and that composites with 30% of TOCNCs showed better performances for both types of dressings in comparison to those with 10% and 50%.

Concerning biological properties, hemostatic evaluation in vivo compared commercial gauze, pure alginate and composites. The composites showed lower bleeding and lower hemostasis time than gauze and alginate dressings for liver and ear injuries. In addition, the composite with 30% of TOCNCs achieved the best performance. The authors mentioned that the charges present on TOCNC's surface could attract and activate platelets; also, the combination with Ca^{2+} cations of crosslinked alginate promoted water absorption from the blood, which may concentrate clotting factors and accelerate clot formation. Moreover, the evaluation of biological degradation demonstrated the complete absorption of the composites with 30% of TOCNCs after 21 days and the stimulation of the growth of new tissue. Thus, the physical and biological properties of TOCNCs/alginate composites can make them promisor materials for wound healing applications (Cheng et al. 2017).

7 Types of wound dressing materials

Dressings are a class of devices of great interest for the biomedical and pharmaceutical fields. Although dressing has been widely disseminated in the literature, numerous discoveries about them and the wound itself have changed their perspective. The big turning point came with discovering that the wound's hot and humid environment provides faster and more successful healing. It is pertinent to note that earlier, the dressings had the function of keeping the wound dry, allowing the exudates from the wound to evaporate and preventing the penetration of harmful bacteria (Boateng et al. 2008).

Furthermore, when developing a new dressing, it must have the ability to absorb exudate during the process, as well as it must not have rigid adherence to repair material on the desiccated wound surface to avoid a new trauma during its removal (Huang et al. 2018).

Based on these characteristics, many dressings have been developed to overcome the disadvantages of traditional dressings and numerous devices have been investigated, such as hydrogels, thin films, ointments, tapes, sponges and many others. However, the choice of a material and its physical properties depends on the type of wound (acute, chronic, exudative or dry wounds, etc.) and on the different stages involved in the healing process, since there is not a single dressing for the management of all types and stages of wound (Boateng et al. 2008).

Cellulose nanocrystals have been demonstrated to be attractive in manufacturing dressings that promote wound healing (Du et al. 2019a; Karimian et al. 2019; Younas et al. 2019; Zubik et al. al. 2017). However, the most suitable polymeric matrix to obtain the best properties of the final material is still the subject of recent studies. Table 2 presents some of the most addressed matrices in recent years.

According to Table 2, the latest research has shown that chitosan is the most studied polymeric matrix for this type of application. Along with their biocompatibility, low

Table 2 Main materials researched for wound dressings with CNCs carried out in the last two decades

Dressing type	Polymeric matrix	Year	References
Thin films	Chitosan	2014	Trigueiro et al. (2014)
Films	Sodium carboxymethyl cellulose	2016	Oun and Rhim (2016)
Films and sponges	Alginate	2017	Shojaeiarani et al. (2019)
Films	Poly(lactic acid)	2017	Pal et al. (2017)
Hydrogels	Poly(N-isopropylacrylamide)	2017	Zubik et al. (2017)
Hydrogels	Cellulose nanocrystals isolated from *Dendrocalamus hamiltonii* and *Bambusa bamboos* leaves	2017	Singla et al. (2017b)
Ointments and films	Cellulose nanocrystals isolated from *Dendrocalamus hamiltonii* and Bambusa *bamboos* leaves	2017	Singla et al. (2017a)
Ointments and strips	Cellulose nanocrystals isolated from *Syzygium cumini* leaves	2017	Singla et al. (2017c)
Films	Chitosan	2018	Dong and Li (2018)
Hydrogels	Carboxymethyl chitosan	2018	Huang et al. (2018)
Filaments	Chitin	2018	Wu et al. (2018a)
Films	Polyvinyl alcohol	2018	Tong et al. (2018)
Films	Chitosan and gelatin	2019	Akhavan-Kharazian and Izadi-Vasafi (2019)
Hydrogels	Solution-mixing of *N,N*-dimethylacrylamide-stat-3-acrylamidophenylboronicacid statistical copolymers and poly(glycerolmonomethacrylate) chains	2019	Du et al. (2019b)

immunogenicity, and biodegradability, the amine groups of chitosan promote its mucoadhesiveness when protonated through electrostatic interactions between the polycation formed and the negatively charged mucus (dependent on the pH of the medium). Furthermore, the great adhesion to mucous tissues results in a process favouring the healing stages (Akhavan-Kharazian and Izadi-Vasafi 2019; Xiang et al. 2020; Yang et al. 2017; Younas et al. 2019).

Regarding the structure, films have been the main type of dressing developed to obtain CNCs materials, mainly due to the ease and low cost of processing. In general, they are obtained by solution casting, which allows obtaining independent films with controllable thicknesses, besides presenting high reproducibility (Lizundia et al. 2020; Younas et al. 2019). Despite some limitations, such as low mechanical resistance and complex handling, hydrogels have notable representativeness among CNC dressings because they can absorb and retain exudate from the wound and maintain an ideal moisture environment for healing while protecting the wound site (Huang et al. 2018; Xiang et al. 2020).

Akhavan-Kharazian and Izadi-Vasafi (2019) studied films based on chitosan, CNCs and calcium peroxide for potential applications as wound dressings. They showed that the association of these materials presented synergistic effects, increased mechanical properties, reduced swelling and increased antibacterial activity. Besides, according to Capozza et al. (2016) the films did not show cytotoxicity and provided an increase in the growth of human fibroblast cells for 7 days.

In addition to the traditional films, Cheng et al. (2017b) developed sponges of nanocrystals of oxidized cellulose with sodium alginate, in the proportion of 30/70% (w/w), which showed high hemostatic efficiency (~70 s) with low blood loss in trauma models of rabbit ear and hepatic artery. Also, these sponges were completely biodegraded without an inflammatory reaction after three weeks.

Regardless of the chosen structure and the desired polymeric matrix, these nanocomposites, aside from being biocompatible, can keep a balance of ambient humidity while preventing the proliferation of unwanted pathogens. Besides the features presented, the proposed material must stimulate the healing process, absorb blood quickly, and be bioabsorbable at an efficient rate for proper wound healing.

8 Biocomposites preparation techniques

Introducing cellulose nanocrystals in natural and synthetic polymer matrices has improved diverse mechanical, thermal, morphological, and biological characteristics. To this end, however, it is important to ensure that the processing method will promote a good dispersion of the nanoparticles in the matrix. In addition, a technique to prepare bio nanocomposites should be compatible with the type of dressing and prevent aggregation of nanofillers. The main techniques used to prepare bionanocomposites with CNCs are solution casting, electrospinning, freeze-drying, and 3D printing.

8.1 Solution casting

The solution casting technique consists of dissolving the two materials in a common solvent, stirring the suspension to achieve a homogeneous phase with a rigid percolating network, and evaporating the solvent to form a solid nanocomposite film (Oksman et al. 2016). The processing parameters that influence the homogeneity of nanocomposites are solubility in the solvent, stirring and evaporation time, temperature and compatibility, which must be adjusted according to the nature of the charge and matrix. Although, for example, water is a common solvent used to prepare nanocomposites with CNCs and water-soluble polymers because of their strong hydrophilic interaction, slow processing can lead to nanocrystals self-organization and formation of percolating networks (Oksman et al. 2016). Temperature selection can be perceived by comparing the studies of Li et al. (2014), who prepared collagen/CNCs films by solution casting stirring the mixture for 24 h and air-drying at room temperature, and Cheng et al. (2017b), who produced alginate/CNCs films through the same method, by stirring the mixture at 60–70 °C for 1 h and oven-drying at 40 °C for two days. In both cases, the parameters were chosen according to the nature of the matrix since collagen is comprised of proteins and should not be exposed to high temperatures, whereas alginate can bear temperature variation.

8.2 Electrospinning

Electrospinning is a recent technique developed in the last two decades used to produce continuous polymer fibers in a diameter scale ranging from nano to micrometric size (Rogina 2014; Bombin et al. 2020). It consists of applying high voltage to overcome the superficial tension of the melted polymer or a polymer solution to form a jet, which is constantly deposited in a collector during the process (Khamforoush et al. 2014a). The polymeric solution is filled into a syringe and flows at a constant rate with the aid of a pump to a feed tube connected to a spinneret (Pilehvar-Soltanahmadi et al. 2018). When the voltage is applied, opposite charges in the spinneret and the collector produce an electrical field (Khamforoush et al. 2015; Bombin et al. 2020). At the end of the spinneret, the polymer droplet changes its shape into a conic by electrical forces since the voltage reaches a high enough value to overcome the superficial tension (Khamforoush et al. 2014b). Thus, the polymeric solution is ejected into the collector and the

solvent evaporates in the process, resulting in an isotropically oriented fiber mat (Megelski et al. 2002; Castro et al. 2021). Three types of parameters influence the properties of the nanofiber mats according to Rogina (2014): solution parameters (viscosity, concentration, molecular weight, surface tension, conductivity, dipole moment, dielectric strength), processing parameters (flow rate, electric field strength, tip-to-collector distance, needle (tip) shape, collector composition and geometry), and finally, ambient parameters including temperature, humidity and airflow. Hivechi et al. (2019) produced gelatin nanofibers with different amounts of CNCs and evaluated their viscosity and conductivity. They observed an increase of viscosity with the concentration of CNCs, which is supposed to increase nanofiber diameters. At the same time, they detected a rise in conductivity with the amount of CNCs, because the extraction with sulfuric acid introduced anionic charges on their surfaces. The increase in conductivity induced a decrease in nanofiber diameters. Thus, the increase of viscosity and conductivity together produced a plateau for nanofibers diameter, which allowed a more homogeneous structure to the mats.

8.3 Freeze-drying

Freeze-drying is a technique to prepare composites with high porosity, and it is based on the principle of producing thermodynamic instability in a system through rapid cooling to cause phase separation and removing the solvent by sublimation (Annabi et al. 2010). The porosity of composites prepared by this technique, also named lyophilization, can be influenced by the cooling rate. A rapid cooling rate leads to uncontrolled nucleation of the ice crystals, and the growth phase of crystallization may not be completed, leading to heterogeneity in the porous structure (O'Brien et al. 2004). Mueller et al. (2015) prepared CNC/PVOH aerogels using two procedures of freeze-drying: submerging the suspension in liquid nitrogen at − 196 °C for 5 min, named as fast-freezing (FF) and storage it in a freezer at − 26 °C for 24 h, referred as slow freezing (SF). The results demonstrate lower elastic modulus values for composites prepared by FF than those made by SF for all compositions. SEM micrographs revealed a sheet-like structure for the FF composites and a three-dimensional structure for the SF aerogels. Therefore, slow freezing can be a favourable procedure to prepare composites for wound dressing by freeze-drying since it improves the mechanical properties and influences the morphology of the porous. As mentioned in this work, improved mechanical properties leads to more stable and resistant materials capable of bearing body stress. While the porous structure can directly influence the blood absorption and, consequently, induce outstanding hemostatic performances.

8.4 3D-printing

3D printing is a group of techniques to fabricate complex structures in three dimensions with high accuracy by depositing the printing material in a patterned way until they reach the desired size, ranging from sub-micrometre to several meters (Farahani et al. 2016). The process involves solidifying the printing material, which can be liquid resins, powders and molten polymers (Farahani and Dubé 2018). The 3D printing of nanocomposites can develop functional materials and tailor their properties for a specific application. The processing parameters are related to the type of technique used to fabricate the nanocomposite. For injection printing, voltage, frequency, nozzle diameter, viscosity, and ink surface tension must be adjusted (Farahani et al. 2016). According to Chen et al. (2018), the inks applied on 3D printing should possess shear-thinning behaviour and recovering properties after printing. During the printing process, the ink materials are subjected to a high pressure to flow through the nozzle. After that, the forces are removed, and the material should maintain its shape and remain stable for a long time.

Hydrogels composed by nanocelluloses have been prepared through 3D bioprinting, a subset of 3D printing techniques that applies a precise layer-by-layer positioning of biological materials, biochemicals and living cells to form 3D structures (Murphy and Atala 2014; Rees et al. 2015; Leppiniemi et al. 2017; Wu et al. 2018a; Jessop et al. 2019; Wei et al. 2020; Monfared et al. 2021).

Rees et al. (2015) constructed a wound dressing by 3D bioprinting technique using oxidized cellulose nanocrystals (CNCs) and nanofibrils (CNF). CNCs gels presented more pronounced shear-thinning behaviour, which is a valuable characteristic of 3D printing. That can be explained due to the facility of CNCs particles to become aligned when shear-stressed.

Jessop et al. (2019) studied bioink formulations using nanocelluloses and alginate and evaluated the printability and cell viability using human nasoseptal chondrocytes. The rheological measurements revealed that all bioink formulations with nanocellulose presented a shear-thinning behaviour since the viscosity decreased with increasing the shear rate. Moreover, unlike pure alginate bioinks, all formulations with nanocellulose exhibited higher storage Moduli (G') than loss Moduli (G"). These results indicated that the insertion of nanocelluloses in alginate bioink formulations might increase their post-printing stability. Finally, the cell viability test showed better performance for bioinks containing nanocelluloses and alginate than the control sample (cell culture in plastic alone).

9 Challenges and perspectives for CNC applications

Although cellulose nanocrystals are recognized as multifunctional materials that can be applied in different areas because of their unique properties and renewable and sustainable sources, the great challenge in their wide use remains on large-scale production. The main source to obtain CNCs is wood, and the process of extraction includes acid hydrolysis with sulfuric acid that is recyclable and cheaper than other acids. The hydrolyzed by-product generated in the reaction can be used to obtain biofuels, but its treatment investments demand high energy and costs (Thomas et al. 2020). Other issues in acid hydrolysis that can increase production prices are its low yield, approximately 50%, and the high capital investment in the drying process due to a large amount of water in the final suspensions (de Assis et al. 2017). The manufacturing cost of CNCs is estimated from 3632 USD/t to 4420 USD/t (dry equivalent), including depreciation costs (de Assis et al. 2017). Besides, the current production is larger than the market demand for the commodity (Nanocellulose Mark 2019). Therefore, efforts have been made to apply readily available sources in their manufactures, such as agricultural biomass and industrial waste, which present economic and ecological benefits (Rajinipriya et al. 2018).

Nevertheless, cellulose nanocrystals are promising nanomaterials for diverse applications such as food packaging, biomedical field, cosmetics, electronics, optical materials, automobile, construction, aerospace, textiles, paper industry and water purification (Reshmy et al. 2020). They have been a competitive material in the nanomaterial market, especially for their mechanical properties comparable to Kevlar and for being extracted from sustainable sources.

There are many companies for CNCs production around the world. CelluForce is a Canadian company leader in CNCs large scale production with 300 tons per year (Celluforce 2021). Their product is available in the market named CelluForce NCC®, and it is obtained by sulfuric acid hydrolysis (Mokhena and John 2020). CelluForce offers its customers various product grades according to their application requirements, which is a prerequisite to being highly competitive in the field (Celluforce 2021). American Process Inc., Imerys-UK and Nippon Paper Industries-Japan are other examples of entities that produce CNCs on a large scale worldwide (Mokhena and John 2020).

For wound healing applications, there are at least three products in the market: wound dressings CelMat®, EpiProtect® and Nanoderm™, all are based on bacterial nanocellulose. The unique properties of this type of nanocellulose are related to its high purity, high degree of crystallinity and 3D nanostructure (Bowil/Biotech 2021).

Napavichayanun et al. (2016) tested the safety of a wound dressing containing bacterial nanocellulose, polyhexamethylene biguanide (PHMB) and sericin in vitro (mouse fibroblast cells), in vivo (implanted subcutaneously in rats), and with clinical studies (normal skin of healthy volunteers to evaluate the irritation). The dressing promoted cell growth and proliferation and demonstrated biocompatibility as good as the commercially available control Bactigras® (0.5% chlorhexidine acetate in soft white paraffin). In addition, good results were achieved for both in vivo and clinical tests. The dressing showed a lower inflammation reaction than the control when implanted in rats, and it did not cause any irritation to the skin of the volunteers.

Meschini et al. (2020) tested the toxicity of CNCs from bleached cellulose pulps obtained by TEMPO-mediated oxidation and the hydrogels produced by crosslinking of CNCs with different cations. CNCs self-assembled did not present cytotoxicity to cell culture (Melanoma A375 and M14) after 24 h of incubation. CNC hydrogels prepared with Ca^{2+} and Mg^{2+} demonstrated high cell viability after 24 h of incubation when soaked in ultra-pure water for five days to remove the unbound cations. However, the mechanical shearing of CNCs hydrogels on cell monolayers decreased the cell viability significantly, and this effect needs to be further investigated.

Besides, inflammatory responses are reported for CNCs applied in vivo and in vitro models, probably due to their high aspect ratio, insolubility and biopersistency (Ventura et al. 2020). Therefore, the safety of this nanomaterial must be examined in detail to apply in clinical studies.

10 Conclusions

This work addresses the application of cellulose nanocrystals to prepare nanocomposites for the specific area of wound healing. Oxidized cellulose is widely applied for this application, but some clinical studies have contested its efficiency and safety. Novel wound dressings have been prepared using nanocomposites with cellulose nanocrystals (CNCs). The CNCs versatility in the preparation of different dressings (films, filaments, hydrogels, ointments and sponges) amplify the range of its applications according to the type of wound. A dressing containing CNCs presented outstanding performances on absorbing fluids and exudates, attributed to their large surface area and hydrophilicity. Enhanced mechanical properties were found in all bionanocomposites presented in this work, confirming the reinforcement properties of this nanomaterial. However, high contents of CNCs in polymeric matrices can cause two undesired effects: the decreasing absorption capacity because they can easily penetrate the porous structure in the matrix; and the flexibility of dressings due to the limitation of chains mobility. The good dispersion

of CNCs in the biopolymers matrices was identified as an important characteristic to achieve the desired properties for the materials. Moreover, the oxidation treatment of CNCs had a significant influence on the hemostatic and biodegradable performance of the dressings. Finally, bionanocomposites with CNCs demonstrated good biocompatibility, promoting cell growth and proliferation, but inflammation reactions need more investigation to prove their safety. Thus, cellulose nanocrystals are a potential option for developing new high-performance wound dressings, but more effort is still required in this direction.

Acknowledgements The authors would like to thank the funding received CNPq (130508/2020-9) and Fundação de Amparo à Pesquisa do Estado de São Paulo—FAPESP (Project No. 2018/18722-6).

Author contributions All the authors contributed to the study conception and design. Idea for the article: LHIM and ACMC. Literature research and data analysis: ACMC and KCdC. Figure design: TH, ACMC, KCdC. Critically revised the work: LZL, TH and LHIM. The authors have no relevant financial or non-financial interests to disclose.

References

T. Adschiri, Y.W. Lee, M. Goto, S. Takami, Green Chem. **13**, 1380 (2011)
P. Agulhon, M. Robitzer, L. David, F. Quignard, Biomacromol **13**, 215 (2012)
N. Akhavan-Kharazian, H. Izadi-Vasafi, Int. J. Biol. Macromol. **133**, 881 (2019)
I.F.H. AI-Jawhari, *Handbook of Nanomaterial Nanocomposites Energy Environmental Applications* (2020), p. 1
M.G. Albu, I. Titorencu, M.V. Ghica, in *Biomaterials Applications for Nanomedicine*, edited by R. Pignatello (InTech, Rijeka, 2011), pp. 333–357
N. Annabi, J.W. Nichol, X. Zhong, C. Ji, S. Koshy, A. Khademhosseini, F. Dehghani, Tissue Eng. Part B Rev. **16**, 371 (2010)
P. Aramwit, *Introduction to Biomaterials for Wound Healing* (Elsevier Ltd, London, 2016)
D. Archana, P.K. Dutta, J. Dutta, *Chitin and Chitosan for Regenerative Medicine* (2016)
D.K. Arserim-Uçar, F. Korel, L.S. Liu, K.L. Yam, Food Chem. **336**, 127597 (2021)
L. Bacakova, J. Pajorova, M. Bacakova, A. Skogberg, P. Kallio, K. Kolarova, V. Svorcik, Nanomaterials **9**, 164 (2019)
B. Balakrishnan, M. Mohanty, P.R. Umashankar, A. Jayakrishnan, Biomaterials **26**, 6335 (2005)
S. Beck-Candanedo, M. Roman, D.G. Gray, Biomacromol **6**, 1048 (2005)
A.M. Behrens, M.J. Sikorski, P. Kofinas, J. Biomed. Mater. Res. Part A **102**, 4182 (2014)
J.S. Boateng, K.H. Matthews, H.N.E. Stevens, G.M. Eccleston, J. Pharm. Sci. **97**, 2892 (2008)
A.D.J. Bombin, N.J. Dunne, H.O. McCarthy, Mater. Sci. Eng. C **114**, 110994 (2020)
Bowil/Biotech (2021)
R. Brandes, L. De Souza, C. Carminatti, D. Recouvreux, Int. J. Nanosci. **19**, 1 (2020)
X. Cao, B. Ding, J. Yu, S.S. Al-deyab, Carbohydr. Polym. **90**, 1075 (2012)
M. Capozza, G. Pansini, A.M. Buccoliero, G. Barbagli, B. Ashraf-Noubari, F. Mariotti, F. Ammannati, Iran. J. Neurosurg. **2**, 20 (2016)
K.C. Castro, M.G.N. Campos, L.H.I. Mei, Int. J. Biol. Macromol. **173**, 251 (2021)
Celluforce (2021)
About CelluForce (2021)
P.R. Chawla, I.B. Bajaj, S.A. Survase, R.S. Singhal, Food Technol. Biotechnol. **47**, 107 (2009)
X. Chen, X. Deng, W. Shen, L. Jiang, BioResources **7**, 4237 (2012)
Y. Chen, Y. Wang, Q. Yang, Y. Liao, B. Zhu, G. Zhao, R. Shen, X. Lu, S. Qu, J. Mater. Chem. B **6**, 4502 (2018)
Y. Chen, L. Wu, P. Li, X. Hao, X. Yang, G. Xi, W. Liu, Y. Feng, H. He, C. Shi, Macromol. Biosci. **1900370**, 1 (2020)
W. Cheng, J. He, Y. Wu, C. Song, S. Xie, Y. Huang, B. Fu, Cellulose **20**, 2547 (2013)
W. Cheng, J. He, M. Chen, D. Li, H. Li, L. Chen, Y. Cao, J. Wang, Y. Huang, Fibers Polym. **17**, 1277 (2016a)
W. Cheng, H. Li, X. Zheng, L. Chen, F. Cheng, J. He, K. Liu, P. Cai, X. Wang, Y. Huang, Phys. Chem. Chem. Phys. **18**, 29183 (2016b)
F. Cheng, C. Liu, X. Wei, T. Yan, H. Li, J. He, Y. Huang, A.C.S. Sustain, Chem. Eng. **5**, 3819 (2017)
B. Cohen, A. Shefy-Peleg, M. Zilberman, J. Biomater. Sci. Polym. Ed. **25**, 224 (2014)
D.S. da Perez, S. Montanari, M.R. Vignon, Biomacromolecules **4**, 1417 (2003)
T. Dai, M. Tanaka, Y.-Y. Huang, M.R. Hamblin, *Chitosan Preparations for Wound-Healing Effects* (2011)
C.A. de Assis, C. Houtman, R. Phillips, E.M.T. Bilek, O.J. Rojas, L. Pal, M.S. Peresin, H. Jameel, R. Gonzalez, Biofuels Bioprod. Biorefining **11**, 682 (2017)
I.A.A. de Fernandes, A.C. Pedro, V.R. Ribeiro, D.G. Bortolini, M.S.C. Ozaki, G.M. Maciel, C.W.I. Haminiuk, Int. J. Biol. Macromol. **164**, 2598 (2020)
B. Deepa, E. Abraham, N. Cordeiro, M. Faria, G. Primc, Y. Pottathara, M. Leskovšek, M. Gorjanc, M. Mozetič, S. Thomas, L.A. Pothan, Heliyon **6**, e03266 (2020)
M. Djabourov, P. Papon, Polymer (guildf) **24**, 537 (1983)
F. Dong, S. Li, Polymers (basel) **10**, 673 (2018)
H. Du, C. Liu, X. Mu, W. Gong, D. Lv, Y. Hong, C. Si, B. Li, Cellulose **23**, 2389 (2016)
L. Du, J. Wang, Y. Zhang, C. Qi, M.P. Wolcott, Z. Yu, Nanomaterials **7**, 1 (2017)
H. Du, W. Liu, M. Zhang, C. Si, X. Zhang, B. Li, Carbohydr. Polym. **209**, 130 (2019a)
W.B. Du, A. Deng, J. Guo, J. Chen, H. Li, Y. Gao, Carbohydr. Polym. **223**, 115084 (2019b)
R.D. Farahani, M. Dubé, D. Therriault, Adv. Mater. **28**, 5794 (2016)
R.D. Farahani, M. Dubé, Adv. Eng. Mater. **20**, 1 (2018)
M. Fazil, S. Nikhat, J. Ethnopharmacol. **257**, 112878 (2020)
E.J. Foster, R.J. Moon, U.P. Agarwal, M.J. Bortner, J. Bras, S. Camarero-Espinosa, K.J. Chan, M.J.D. Clift, E.D. Cranston, S.J. Eichhorn, D.M. Fox, W.Y. Hamad, L. Heux, B. Jean, M. Korey, W. Nieh, K.J. Ong, M.S. Reid, S. Renneckar, R. Roberts, J.A. Shatkin, J. Simonsen, K. Stinson-Bagby, N. Wanasekara, J. Youngblood, Chem. Soc. Rev. **47**, 2609 (2018)
A. Gaspar-Pintiliescu, A.M. Stanciuc, O. Craciunescu, Int. J. Biol. Macromol. **138**, 854 (2019)
C. Ghobril, M.W. Grinstaff, Chem. Soc. Rev. **44**, 1820 (2015)
L. Golbaghi, M. Khamforoush, T. Hatami, Carbohydr. Polym. **174**, 780 (2017)
A.C.D.O. Gonzalez, Z.D.A. Andrade, T.F. Costa, A.R.A.P. Medrado, An. Bras. Dermatol. **91**, 614 (2016)
S. Gopi, P. Balakrishnan, D. Chandradhara, D. Poovathankandy, S. Thomas, Mater. Today Chem. **13**, 59 (2019)
M.F.P. Graça, S.P. Miguel, C.S.D. Cabral, I.J. Correia, Carbohydr. Polym. **241**, 116364 (2020)

Y. Habibi, L.A. Lucia, O.J. Rojas, Chem. Rev. **110**, 3479 (2010)
D.M. Hariyadi, N. Islam, Adv. Pharmacol. Pharm. Sci. **2020**, 1 (2020)
T. Hatami, J. Vigano, L.H.I. Mei, J. Martinez, J. Supercrit. Fluids **160**, 104791 (2020)
S.S.Z. Hindi, Nanosci. Nanotechnol. Res. **4**, 17 (2017)
A. Hivechi, S. Hajir Bahrami, R.A. Siegel, Int. J. Biol. Macromol. **124**, 411 (2019)
W. Huang, Y. Wang, Z. Huang, X. Wang, L. Chen, Y. Zhang, L. Zhang, A.C.S. Appl, Mater. Interfaces **10**, 41076 (2018)
R.W. Hutchinson, K. George, D. Johns, L. Craven, G. Zhang, P. Shnoda, Cellulose **20**, 537 (2013)
A. Isogai, T. Saito, H. Fukuzumi, Nanoscale **3**, 71 (2011)
Z.M. Jessop, A. Al-Sabah, N. Gao, S. Kyle, B. Thomas, N. Badiei, K. Hawkins, I.S. Whitaker, Biofabrication **11**, 045006 (2019)
A.F. Jozala, L.C. de Lencastre-Novaes, A.M. Lopes, V. de Carvalho Santos-Ebinuma, P.G. Mazzola, A. Pessoa, D. Grotto, M. Gerenutti, M.V. Chaud, Appl. Microbiol. Biotechnol. **100**, 2063 (2016)
H. Kargarzadeh, M. Mariano, D. Gopakumar, I. Ahmad, S. Thomas, A. Dufresne, J. Huang, N. Lin, *Advances in Cellulose Nanomaterials* (Springer, Netherlands, 2018)
A. Karimian, H. Parsian, M. Majidinia, M. Rahimi, S.M. Mir, H. Samadi Kafil, V. Shafiei-Irannejad, M. Kheyrollah, H. Ostadi, B. Yousefi, Int. J. Biol. Macromol. **133**, 850 (2019)
H.P.S.A. Khalil, Y. Davoudpour, M.N. Islam, A. Mustapha, K. Sudesh, R. Dungani, M. Jawaid, Carbohydr. Polym. **99**, 649 (2014)
M. Khamforoush, T. Asgari, T. Hatami, F. Dabirian, Korean J. Chem. Eng. **31**, 1695 (2014a)
M. Khamforoush, T. Hatami, M. Mahjob, F. Dabirian, A. Zandi, Iran. Polym. J. (english Ed.) **23**, 569 (2014b)
M. Khamforoush, O. Pirouzram, T. Hatami, Desalination **359**, 14 (2015)
H. Khoshmohabat, S. Paydar, A. Makarem, M.Y. Karami, N. Dastgheib, S.A.H. Zahraei, R. Rezaei, G. Sadat, M. Nezhad, Open Access. Emerg. Med. **11**, 171 (2019)
S. S. Kordestani, in *Atlas of Wound Healing* (Elsevier, 2019), pp. 11–22
A.J. Kuijpers, G.H.M. Engbers, J. Feijen, S.C. De Smedt, T.K.L. Meyvis, J. Demeester, J. Krijgsveld, S.A.J. Zaat, J. Dankert, Macromolecules **32**, 3325 (1999)
K. Leppänen, S. Andersson, M. Torkkeli, M. Knaapila, N. Kotelnikova, R. Serimaa, Cellulose **16**, 999 (2009)
J. Leppiniemi, P. Lahtinen, A. Paajanen, R. Mahlberg, S. Metsä-Kortelainen, T. Pinomaa, H. Pajari, I. Vikholm-Lundin, P. Pursula, V.P. Hytönen, A.C.S. Appl, Mater. Interfaces **9**, 21959 (2017)
A.C.W. Leung, S. Hrapovic, E. Lam, Y. Liu, K.B. Male, K.A. Mahmoud, J.H.T. Luong, Small **7**, 302 (2011)
W. Li, R. Guo, Y. Lan, Y. Zhang, W. Xue, Y. Zhang, J. Biomed. Mater. Res. Part A **102**, 1131 (2014)
N. Lin, J. Huang, P.R. Chang, L. Feng, J. Yu, Coll. Surf. B Biointerfaces **85**, 270 (2011)
L.Z. Linan, A.C.M. Cidreira, C.Q. da Rocha, F.F. de Menezes, G.J. de M. Rocha, A.E.M. Paiva, J. Bioresour. Bioprod. **1** (2021). https://doi.org/10.1016/j.jobab.2021.04.007
J. Liu, S. Willför, A. Mihranyan, Carbohydr. Polym. **172**, 11 (2017)
R. Liu, L. Dai, C. Si, Z. Zeng, Carbohydr. Polym. **195**, 63 (2018)
W. Liu, H. Du, H. Liu, H. Xie, T. Xu, X. Zhao, Y. Liu, X. Zhang, C. Si, A.C.S. Sustain, Chem. Eng. **8**, 16691 (2020)
E. Lizundia, D. Puglia, T.D. Nguyen, I. Armentano, Prog. Mater. Sci. **112**, 100668 (2020)
E.P.C.G. Luz, P.H.S. Chaves, L.A.P. de Vieira, S.F. Ribeiro, M.F. Borges, F.K. Andrade, C.R. Muniz, A.I. Molina, E.R. Castellón, M.F. de Rosa, R.S. Vieira, Carbohydr. Polym. **237**, 116174 (2020)
B. Martina, K. Kateřina, R. Miloslava, G. Jan, M. Ruta, Adv. Polym. Technol. **28**, 199 (2009)
E. Mascheroni, R. Rampazzo, M.A. Ortenzi, G. Piva, S. Bonetti, L. Piergiovanni, Cellulose **23**, 779 (2016)
E. Masci, G. Faillace, M. Longoni, B.M.C. Res, Notes **11**, 3 (2018)
S. Megelski, J.S. Stephens, D. Bruce Chase, J.F. Rabolt, Macromolecules **35**, 8456 (2002)
S. Meschini, E. Pellegrini, C.A. Maestri, M. Condello, P. Bettotti, G. Condello, M. Scarpa, J. Biomed. Mater. Res. Part B Appl. Biomater. **108**, 687 (2020)
A. Mihranyan, J. Appl. Polym. Sci. **119**, 2449 (2010)
K. Missoum, M.N. Belgacem, J. Bras, Materials (basel) **6**, 1745 (2013)
A. Moeini, P. Pedram, P. Makvandi, M. Malinconico, G. Gomez dAyala, Carbohydr. Polym. **233**, 115839 (2020)
T.C. Mokhena, M.J. John, Cellulose **27**, 1149 (2020)
M. Monfared, D. Mawad, J. Rnjak-Kovacina, and M. H. Stenzel, J. Mater. Chem. B. **9,** 6163–6175 (2021)
S. Montanari, M. Roumani, L. Heux, M.R. Vignon, Macromolecules **38**, 1665 (2005)
J. Moohan, S. A. Stewart, E. Espinosa, A. Rosal, A. Rodríguez, E. Larrañeta, R. F. Donnelly, and J. Domínguez-Robles, Appl. Sci. **10** (2020)
R. J. Moon, A. Martini, J. Nairn, J. Simonsen, and J. Youngblood, *Cellulose Nanomaterials Review: Structure, Properties and Nanocomposites* (2011)
S. Mueller, J. Sapkota, A. Nicharat, T. Zimmermann, P. Tingaut, C. Weder, E.J. Foster, J. Appl. Polym. Sci. **132**, 1 (2015)
S.V. Murphy, A. Atala, Nat. Biotechnol. **32**, 773 (2014)
K. J. Nagarajan, N. R. Ramanujam, M. R. Sanjay, S. Siengchin, B. S. Rajan, K. S. Basha, P. Madhu, and G. R. Raghav, Polym. Compos. **1,** 1588–1630 (2021)
P. Nakielski, F. Pierini, Acta Biomater. **84**, 63 (2019)
Nanocellulose Mark. Prod. an Pricing Rep. 2019 (2019)
S. Napavichayanun, R. Yamdech, P. Aramwit, Arch. Dermatol. Res. **308**, 123 (2016)
D.M.D. Nascimento, J.S. Almeida, M.S. do Vale, R.C. Leitão, C.R. Muniz, M.C.B.D. Figueirêdo, J.P.S. Morais, M.F. de Rosa, Ind. Crops Prod. **93**, 66 (2016)
N. Naseri, A.P. Mathew, L. Girandon, M. Frohlich, K. Oksman, Cellulose **22**, 521 (2015)
T.T. Nge, S.H. Lee, T. Endo, Cellulose **20**, 1841 (2013)
L.P. Novo, J. Bras, A. García, N. Belgacem, A.A.S. Curvelo, A.C.S. Sustain, Chem. Eng. **3**, 2839 (2015)
L.P. Novo, J. Bras, A. García, N. Belgacem, A.A.S. da Curvelo, Ind. Crops Prod. **93**, 88 (2016)
F.J. O'Brien, B.A. Harley, I.V. Yannas, L. Gibson, Biomaterials **25**, 1077 (2004)
S. Ohta, T. Nishiyama, M. Sakoda, K. Machioka, M. Fuke, S. Ichimura, F. Inagaki, A. Shimizu, K. Hasegawa, N. Kokudo, M. Kaneko, Y. Yatomi, T. Ito, J. Biosci. Bioeng. **119**, 718 (2015)
K. Oksman, Y. Aitomäki, A.P. Mathew, G. Siqueira, Q. Zhou, S. Butylina, S. Tanpichai, X. Zhou, S. Hooshmand, Compos. Part A Appl. Sci. Manuf. **83**, 2 (2016)
F. Ostadhossein, N. Mahmoudi, G. Morales-Cid, E. Tamjid, F.J. Navas-Martos, B. Soriano-Cuadrado, J.M.L. Paniza, A. Simchi, Materials (basel) **8**, 6401 (2015)
A.A. Oun, J.W. Rhim, Carbohydr. Polym. **150**, 187 (2016)
J. Oyama, Á.C. Fernandes Herculano Ramos-Milaré, D.S.S. Lopes Lera-Nonose, V. Nesi-Reis, I. Galhardo Demarchi, S.M. Alessi Aristides, J. Juarez Vieira Teixeira, T. Gomes Verzignassi Silveira, M.V. Campana Lonardoni, Photodiagn. Photodyn. Ther. **30**, 101682 (2020)
N. Pal, P. Dubey, P. Gopinath, K. Pal, Int. J. Biol. Macromol. **95**, 94 (2017)
B. Pereira, V. Arantes, Ind. Crops Prod. **152**, 112377 (2020)
P.H.F. Pereira, H.O.J. Luiz, L.V. Coutinho, B. Duchemin, M.O.H. Cioffi, Cellulose **27**, 5745 (2020)

Y. Pilehvar-Soltanahmadi, M. Dadashpour, A. Mohajeri, A. Fattahi, R. Sheervalilou, N. Zarghami, Mini-Reviews. Med. Chem. **18**, 414 (2018)
G.N. Piozzi, E. Reitano, V. Panizzo, B. Rubino, D. Bona, D. Tringali, G. Micheletto, Am. J. Case Rep. **19**, 812 (2018)
R. Poonguzhali, S.K. Basha, V.S. Kumari, Int. J. Biol. Macromol. **112**, 1300 (2018)
M. Rajinipriya, M. Nagalakshmaiah, M. Robert, S. Elkoun, A.C.S. Sustain, Chem. Eng. **6**, 2807 (2018)
A. Rees, L.C. Powell, G. Chinga-Carrasco, D.T. Gethin, K. Syverud, K.E. Hill, D.W. Thomas, Biomed Res. Int. **2015**, 1–7 (2015)
R. Reshmy, E. Philip, S. A. Paul, A. Madhavan, R. Sindhu, P. Binod, A. Pandey, and R. Sirohi, Rev. Environ. Sci. Bio/Technology (2020)
N. Rhein-Knudsen, M.T. Ale, A.S. Meyer, Mar. Drugs **13**, 3340 (2015)
A.P.H. Rodrigues, S.D. de Souza, C.S.B. Gil, F.V. Pereira, L.C.A. de Oliveira, P.S. de Oliveira Patricio, J. Appl. Polym. Sci. **134**, 16 (2017)
A. Rogina, Appl. Surf. Sci. **296**, 221 (2014)
R. Rohaizu, W.D. Wanrosli, Ultrason. Sonochem. **34**, 631 (2017)
T. Saito, I. Shibata, A. Isogai, N. Suguri, N. Sumikawa, Carbohydr. Polym. **61**, 414 (2005)
T. Saito, Y. Okita, T.T. Nge, J. Sugiyama, A. Isogai, Carbohydr. Polym. **65**, 435 (2006)
A. Sbiai, H. Kaddami, H. Sautereau, A. Maazouz, E. Fleury, Carbohydr. Polym. **86**, 1445 (2011)
F.T. Seta, X. An, L. Liu, H. Zhang, J. Yang, W. Zhang, S. Nie, S. Yao, H. Cao, Q. Xu, Y. Bu, H. Liu, Carbohydr. Polym. **234**, 115942 (2020)
U.A. Sezer, İ Sahin, B. Aru, H. Olmez, G.Y. Demirel, S. Sezer, Carbohydr. Polym. **219**, 87 (2019)
J. Shojaeiarani, D. Bajwa, A. Shirzadifar, Carbohydr. Polym. **216**, 247 (2019)
R. Singla, S. Soni, P.M. Kulurkar, A. Kumari, S. Mahesh, V. Patial, Y.S. Padwad, S.K. Yadav, Carbohydr. Polym. **155**, 152 (2017a)
R. Singla, S. Soni, V. Patial, P.M. Kulurkar, A. Kumari, S. Mahesh, Y.S. Padwad, S.K. Yadav, Int. J. Biol. Macromol. **105**, 45 (2017b)
R. Singla, S. Soni, V. Patial, P.M. Kulurkar, A. Kumari, S. Mahesh, Y.S. Padwad, S.K. Yadav, Sci. Rep. **7**, 1 (2017c)
P. Slezak, X. Monforte, J. Ferguson, S. Sutalo, H. Redl, H. Gulle, D. Spazierer, J. Mater. Sci. Mater. Med. **71**, 1 (2018)
M. Smyth, A. García, C. Rader, E.J. Foster, J. Bras, Ind. Crops Prod. **108**, 257 (2017)
P. Sukyai, P. Anongjanya, N. Bunyahwuthakul, K. Kongsin, N. Harnkarnsujarit, U. Sukatta, R. Sothornvit, R. Chollakup, Food Res. Int. **107**, 528 (2018)
M. Tavakolian, S.M. Jafari, T.G.M. Van De Ven, Nano-Micro Lett. **73**, 23 (2020)
H.L. Teo, R.A. Wahab, Int. J. Biol. Macromol. **161**, 1414 (2020)
P. Thomas, T. Duolikun, N.P. Rumjit, S. Moosavi, C.W. Lai, M.R. Bin Johan, L.B. Fen, J. Mech. Behav. Biomed. Mater. **110**, 103884 (2020)
W.Y. Tong, A.Y.K. Bin Abdullah, N.A.S. Binti Rozman, M.I.A. Bin Wahid, M.S. Hossain, L.C. Ring, Y. Lazim, W.N. Tan, Cellulose **25**, 631 (2018)
D. Trache, M.H. Hussin, M.K.M. Haafiz, V.K. Thakur, Nanoscale **9**, 1763 (2017)
J.P.C. Trigueiro, G.G. Silva, F.V. Pereira, R.L. Lavall, J. Colloid Interface Sci. **432**, 214 (2014)
B.D. Ulery, L.S. Nair, C.T. Laurencin, J. Polym. Sci. Part B Polym. Phys. **49**, 832 (2011)
O.M. Vanderfleet, D.A. Osorio, E.D. Cranston, Philos. Trans. A **376**, 20170041 (2018)
K. Varaprasad, T. Jayaramudu, V. Kanikireddy, C. Toro, E.R. Sadiku, Carbohydr. Polym. **236**, 116025 (2020)
N.F. Vasconcelos, J.P.A. Feitosa, F.M.P. da Gama, J.P.S. Morais, F.K. Andrade, M.S.M. de Souza Filho, M.F. de Rosa, Carbohydr. Polym. **155**, 425 (2017)
C. Ventura, F. Pinto, A. F. Lourenço, P. J. T. Ferreira, H. Louro, and M. J. Silva, *On the Toxicity of Cellulose Nanocrystals and Nanofibrils in Animal and Cellular Models* (2020)
T. Wang, Q. Gu, J. Zhao, J. Mei, M. Shao, Y. Pan, J. Zhang, H. Wu, Z. Zhang, F. Liu, Int. J. Clin. Exp. Pathol. **8**, 6636 (2015)
B. Wang, X. Lv, S. Chen, Z. Li, X. Sun, C. Feng, H. Wang, Y. Xu, Cellulose **23**, 3187 (2016)
T. Wang, Y. Zheng, Y. Shi, L. Zhao, Drug Deliv. Transl. Res. **9**, 227 (2019)
J. Wei, B. Wang, Z. Li, Z. Wu, M. Zhang, N. Sheng, Q. Liang, H. Wang, S. Chen, Carbohydr. Polym. **238**, 116207 (2020)
H. Wu, G.R. Williams, J. Wu, J. Wu, S. Niu, H. Li, H. Wang, L. Zhu, Carbohydr. Polym. **180**, 304 (2018a)
Y. Wu, F. Wang, Y. Huang, Clin. Appl. Thromb. **24**, 566 (2018b)
Q. Xiang, Y.Y. Lee, P.O. Pettersson, R.W. Torget, Appl. Biochem. Biotechnol. **105**, 505 (2003)
J. Xiang, L. Shen, Y. Hong, Eur. Polym. J. **130**, 109609 (2020)
X. Yang, W. Liu, N. Li, M. Wang, B. Liang, I. Ullah, A. Luis Neve, Y. Feng, H. Chen, C. Shi, Biomater. Sci. **5**, 2357 (2017)
F. Yin, L. Lin, S. Zhan, J. Biomater. Sci. Polym. Ed. **30**, 190 (2019)
M. Younas, A. Noreen, A. Sharif, A. Majeed, A. Hassan, S. Tabasum, A. Mohammadi, K.M. Zia, Int. J. Biol. Macromol. **124**, 591 (2019)
H. Yuan, L. Chen, F.F. Hong, A.C.S. Appl, Mater. Interfaces **12**, 3382 (2020)
K. Zhang, P. Sun, H. Liu, S. Shang, J. Song, D. Wang, Carbohydr. Polym. **138**, 237 (2016)
S. Zhang, J. Li, S. Chen, X. Zhang, J. Ma, J. He, Carbohydr. Polym. **230**, 115585 (2020)
J. Zhao, S. Li, Y. Zhao, Z. Peng, Polym. Bull. **77**, 4401 (2020)
Y. Zhou, T. Saito, L. Bergström, A. Isogai, Biomacromol **19**, 633 (2018)
K. Zubik, P. Singhsa, Y. Wang, H. Manuspiya, R. Narain, Polymers (basel) **9**, 119 (2017)